



UNIVERSITI PUTRA MALAYSIA

***DEVELOPMENT OF NON-BOUNDARY-FITTED CARTESIAN GRID
METHOD FOR NUMERICAL SIMULATION OF MECHANICAL HEART
VALVE AND THE POTENTIAL FOR BLOOD CLOTTING***

MOHAMAD SHUKRI BIN ZAKARIA

FK 2018 95



**DEVELOPMENT OF NON-BOUNDARY-FITTED CARTESIAN GRID
METHOD FOR NUMERICAL SIMULATION OF MECHANICAL HEART
VALVE AND THE POTENTIAL FOR BLOOD CLOTTING**

By

MOHAMAD SHUKRI BIN ZAKARIA

**Thesis Submitted to the School of Graduate Studies, Universiti Putra Malaysia, in
Fulfilment of the Requirements for the Degree of Doctor of Philosophy**

April 2018

COPYRIGHT

All material contained within the thesis, including without limitation text, logos, icons, photographs and all other artwork, is copyright material of Universiti Putra Malaysia unless otherwise stated. Use may be made of any material contained within the thesis for non-commercial purposes from the copyright holder. Commercial use of material may only be made with the express, prior, written permission of Universiti Putra Malaysia.

Copyright ©Universiti Putra Malaysia



Abstract of thesis presented to the Senate of Universiti Putra Malaysia in fulfilment of the requirement for the degree of Doctor of Philosophy

**DEVELOPMENT OF NON-BOUNDARY-FITTED CARTESIAN GRID
METHOD FOR NUMERICAL SIMULATION OF MECHANICAL HEART
VALVE AND THE POTENTIAL FOR BLOOD CLOTTING**

By

MOHAMAD SHUKRI BIN ZAKARIA

April 2018

Chairman : Kamarul Arifin bin Ahmad, PhD
Faculty : Engineering

Computational fluid dynamics (CFD) simulations are becoming a reliable tool in understanding disease progression, investigating blood flow patterns and evaluating medical device performance such as mechanical heart valves (MHV). Previous studies indicated that the non-physiological flow pattern (i.e. recirculation, stagnation, and vortex) might cause a trapped platelet and be responsible for the formation of blood clots in MHV. Accurate simulation of this flow requires a high order accuracy numerical scheme together with a scale resolving turbulence model such as large eddy simulation (LES). This requires the use of uniform orthogonal grids for the discretisation process, which is not able to handle complex branching arterial domains that contain MHV, where the generation are usually boundary-fitted (BF) grid with non-orthogonality and distortions. Therefore, non-boundary fitted (NBF) Cartesian grid method is an alternative solution. The objective of this study is to develop a new NBF method based on the volume of fluid (VOF), containing the colour function, namely NBF-VOF Cartesian grid method. A single set of governing equation is used for both solid and fluids identified by unity colour function and zero colour function respectively. The solid was treated as a fluid with very high viscosity to theoretically reduce its deformability, and subsequently satisfy a no-slip condition at the boundary. In the first attempt, we found that in prior, the treatment was not satisfied. To suppress the fluid velocities in the solid, we introduced the artificial term derived from the colour function into an algebraic system of momentum equations, which had a significant impact on the originality of this study. The developed solver, NBF-VOF, is then thoroughly validated using a variety of numerical and experimental results available in the literature which is Hagen-Poiseuille flow, lid-driven cavity, flow over a cylinder, 90° tube flow, and pulsatile flow through the real anatomic aorta. Opensource CFD software was used as our simulation platform. Although the second order method degenerates the spatial accuracy of convergence rate as function of the grid size from 2 to 1.5, an agreement was found for all cases qualitative and quantitatively. The grid uncertainty obtained was

less than 5%, which was within the acceptable range. The computational time was lower when the viscosity of solid was higher. However, higher solid viscosity gives lagging in the result for transient cases. Despite this, using higher time step, until the maximum Courant number of 4.0, can speed up the simulation time and preserved the stability. Finally, another breakthrough in this study was the application of the solver to simulate pulsatile blood flow of MHV placed in an axisymmetric and real patient anatomic aorta with the sinus, which reveals complex blood flow patterns, shear stress loading, and history of particles age in the local domain, that consequently can identified the potential of blood clotting.



Abstrak tesis yang dikemukakan kepada Senat Universiti Putra Malaysia sebagai memenuhi keperluan untuk ijazah Doktor Falsafah

PEMBANGUNAN KAEDAH GRID-TIDAK-TERIKAT UNTUK SIMULASI BERANGKA PADA INJAP JANTUNG MEKANIKAL DAN POTENSI UNTUK PEMBEKUAN DARAH

Oleh

MOHAMAD SHUKRI BIN ZAKARIA

April 2018

Pengerusi : Kamarul Arifin bin Ahmad, PhD
Fakulti : Kejuruteraan

Pengkomputeran dinamik bendalir (CFD) telah menjadi alat yang boleh dipercayai dalam memahami perkembangan penyakit, menyiasat corak aliran darah dan menilai prestasi peranti perubatan seperti injap jantung mekanikal (MHV). Kajian terdahulu menunjukkan bahawa corak aliran bukan fisiologi, menyebabkan platelet terperangkap, bertanggungjawab ke atas pembentukan darah beku pada MHV. Ketepatan simulasi aliran ini memerlukan darjah ketepatan yang tinggi dengan skala yang dapat menyelesaikan masalah pergolakan seperti simulasi eddy besar (LES). Ini memerlukan penggunaan grid ortogonal seragam, yang tidak dapat dikendalikan oleh bentuk arteri yang kompleks yang mengandungi MHV, di mana grid biasanya digunakan adalah kaedah grid terikat (BF) yang tidak ortogonal dan terherot. Oleh itu, kaedah grid tidak terikat (NBF) adalah penyelesaian alternatif. Objektif kajian ini adalah untuk membangunkan kaedah NBF baru berdasarkan jumlah cecair (VOF) yang mengandungi warna berfungsi diberi nama NBF-VOF. Satu persamaan digunakan untuk mengenali kedua-dua pepejal dan bendalir adalah melalui warna fungsi uniti dan kosong. Pepejal dianggap sebagai bendalir dengan kelikatan yang sangat tinggi yang secara teorinya mengurangkan perubahan bentuk, dan memenuhi syarat tidak-slip di sempadan. Pada percubaan awal, kami dapati bahawa, kaedah itu tidak memuaskan. Untuk terus menyekat halaju bendalir dalam pepejal, kami memperkenalkan istilah buatan yang diterbitkan dari warna fungsi ke dalam sistem algebra persamaan momentum. Seterusnya, kaedah NBF-VOF disahkan menggunakan pelbagai hasil kaedah berangka dan eksperimen yang terdapat dalam literatur melalui perisian sumber terbuka OpenFoam. Aliran Hagen-poiseuille, rongga yang didorong, aliran ke atas silinder, 90° aliran tiub, dan aliran denyutan melalui aorta anatomik sebenar. Kesamaan yang sangat baik telah dihasilkan untuk semua kes. Walaupun menggunakan ketepatan kaedah darjah kedua, ketepatan kadar konvergen kaedah NBF-VOF berbanding saiz grid merosot daripada 2.0 kepada 1.5, perbandingan yang hampir dengan ujikaji diperoleh dari segi kualitatif dan kuantitatif. The grid uncertainty obtained was less than 5%, which was within the ac-

ceptable range. Ketidakpastian grid diperoleh $< 5\%$, berada pada anggaran yang boleh diterima. Masa pengiraan adalah rendah apabila menggunakan kelikatan pepejal yang tinggi. Tetapi kelikatan pepejal yang tinggi memberikan hasil yang ketinggalan untuk kes bergantung masa. Nisbah kelikatan antara pepejal dan cecair pada magnitud 100, memberikan keadaan optimum untuk kestabilan dan masa pengaliran. Walaubagaimanapun, menggunakan nombor Courant setinggi $Co = 4$, dapat mempercepatkan masa simulasi. Akhirnya, aplikasi kaedah ini telah dijalankan untuk mensimulasikan aliran darah MHV yang diletakkan dalam aorta simetri dan anatomik, yang mendedahkan corak aliran darah yang kompleks, beban tekanan ricih, dan tempoh masa sejarah zarah di domain setempat, yang seterusnya dapat mengenal pasti potensi pembekuan darah.



ACKNOWLEDGEMENTS

My deepest gratitude to my wife, Haslina Abdullah for her love and unwavering support throughout my entire graduate education, particularly toward the end. Her presence was the source of strength and inspiration for me to complete this thesis in which I will be eternally grateful. I am also thankful to my sons Faris, Firas, Faiq for their tears and laughter, which provided me a soothing comfort after those long hard days at work.

I owe a huge amount of gratitude to my committee members, especially to Associate Professor Dr. Ir. Kamarul Arifin Ahmad for sharing with me his knowledge, craftsmanship and wisdom in conducting scientific research. It has been a privilege to be his student. Special thanks to Associate Professor Dr. Farzad for being co-supervisor, and mentor for CFD. In addition, he also showed me the essentials of effective oral and written scientific presentations. To my other committee member, Professor Dr. Masaaki Tamagawa, whose providing Japanese style of guidance, Associate Professor Dr. Ahmad Fazli Abdul Aziz, for providing clinical discussion and medical data, and Associate Professor Dr. Surjatin Wiriadidjaja for his advise on managing research , and the continues supporting guidance. Many thanks also to all my friends and colleagues, such as Dr Zuber, Adi Azriff, Vizy Nazira, Syed Aftab, Mohd Firdaus, and Ernnie Illyani, for their support and lively conversations. I am unable to mention all other names because the list will simply be too long.

Particular thanks to Universiti Putra Malaysia providing the High performance Computing (HPC) facilities. Finally, great appreciation must be extended to the Universiti Teknikal Malaysia Melaka, and Ministry of Higher Education Malaysia for providing the financial means for my graduate education. Without their generous support, this thesis would have never been written.

This thesis was submitted to the Senate of Universiti Putra Malaysia and has been accepted as fulfilment of the requirement for the degree of Doctor of Philosophy. The members of the Supervisory Committee were as follows:

Kamarul Arifin bin Ahmad, PhD

Associate Professor, Ir.
Faculty of Engineering
Universiti Putra Malaysia
(Chairman)

Surjatin Wiriadidjaja, PhD

Associate Professor
Faculty of Engineering
Universiti Putra Malaysia
(Member)

Ahmad Fazli Abdul Aziz, PhD

Associate Professor
Faculty of Medicine and Health Sciences
Universiti Putra Malaysia
(Member)

Farzad Ismail, PhD

Associate Professor
School of Aerospace Engineering
Universiti Sains Malaysia
(Member)

Masaaki Tamagawa, PhD

Professor
Kyushu Institute of Technology
Japan
(Member)

ROBIAH BINTI YUNUS, PhD

Professor and Dean
School of Graduate Studies
Universiti Putra Malaysia

Date:

TABLE OF CONTENTS

| | Page |
|----------------------------------------------------------------------|--------------|
| ABSTRACT | i |
| ABSTRAK | iii |
| ACKNOWLEDGEMENTS | v |
| APPROVAL | vi |
| LIST OF TABLES | xiii |
| LIST OF FIGURES | xiv |
| LIST OF ABBREVIATIONS | xx |
| CHAPTER | |
| 1 INTRODUCTION | 1 |
| 1.1 Motivation | 1 |
| 1.2 Computational Modelling of Cardiovascular Flow | 3 |
| 1.3 Problem Statement | 5 |
| 1.4 Research Objectives | 6 |
| 1.5 Scopes of the Studies | 7 |
| 1.6 Thesis Outline | 8 |
| 2 LITERATURE REVIEW | 9 |
| 2.1 Overview | 9 |
| 2.2 Fluid Dynamics of Mechanical Heart Valve (MHV) on Blood Clotting | 11 |
| 2.2.1 Role of Local Flow in Blood Clotting | 14 |
| 2.2.2 Method for Estimating Blood Clotting | 17 |
| 2.3 Numerical Methods | 19 |
| 2.3.1 Boundary Fitted Method | 19 |
| 2.3.2 Non-Boundary-Fitted Methods | 20 |
| 2.3.3 Mathematical Model for Non-Boundary-Fitted Methods | 28 |
| 2.4 Discretization of a General Scalar Transport Equation | 31 |
| 2.4.1 Discretisation of Spatial Terms | 32 |
| 2.4.2 Temporal Discretization | 35 |
| 2.5 Turbulence Model | 35 |
| 2.5.1 Turbulence Modelling in Mechanical Heart Valve | 37 |
| 2.6 FSI on Blood Clot Estimation | 40 |
| 2.7 Experimental Fluid Dynamics (EFD) for validation | 41 |
| 2.8 Parametric MHV Study | 43 |
| 2.8.1 Effects of Anatomical Model | 43 |
| 2.8.2 Effects of Leaflet Dynamics | 45 |
| 2.8.3 Effects of Valve Orientation | 49 |
| 2.9 Issues and Current Research Directions | 51 |

| | | |
|----------|----------------------------------------------------------------------------------------|------------|
| 2.10 | Summary | 52 |
| 3 | MATHEMATICAL MODELS AND NUMERICAL METHODS | 61 |
| 3.1 | Overview | 61 |
| 3.2 | New NBF-VOF Cartesian Grid Method | 61 |
| 3.2.1 | Treatment I: Setting up high solid viscosity ($\mu_s \rightarrow \infty$) | 63 |
| 3.2.2 | Treatment II: Introducing Artificial Term to the Systems of Linear Algebraic Equations | 64 |
| 3.2.3 | Stability | 66 |
| 3.2.4 | Numerical Experiment of New Developed Method | 70 |
| 3.3 | Choices of Numerical Scheme | 78 |
| 3.4 | Role of Compressive Term | 81 |
| 3.5 | Numerical Algorithm Step | 82 |
| 3.6 | Image-to-Computation Framework | 85 |
| 3.7 | Implementing and Numerical Setup in OpenFOAM | 86 |
| 3.8 | Validation and Verification | 87 |
| 3.9 | Solver Verification | 89 |
| 3.9.1 | Hagen-Poiseuille Flow | 90 |
| 3.9.2 | Lid-Driven Cavity with Embedded Solid | 94 |
| 3.10 | Solver Validation | 97 |
| 3.10.1 | Lid-driven cavity | 97 |
| 3.10.2 | Flow Over a Cylinder in a Free Stream | 99 |
| 3.10.3 | Flow Over a Cylinder Asymmetrically Placed in a Channel | 104 |
| 3.10.4 | Flow on a 90° Tube Bend | 107 |
| 3.11 | Patient Specific Aorta Flow | 109 |
| 3.12 | Summary | 118 |
| 4 | NUMERICAL SIMULATION OF MECHANICAL HEART VALVE | 121 |
| 4.1 | Overview | 121 |
| 4.2 | Computational Setup | 123 |
| 4.2.1 | MHV Placed in Axisymmetric Aorta | 125 |
| 4.2.2 | MHV Placed in Anatomic Aorta | 127 |
| 4.3 | Results and Discussions | 130 |
| 4.3.1 | Validation on Steady Flow: Quantitative Comparison | 130 |
| 4.3.2 | Validation on Pulsatile Flow: Qualitative Comparison | 133 |
| 4.3.3 | Flow Analysis and Aerodynamic Characteristics on Blood Clot Potential | 135 |
| 4.4 | Summary | 151 |
| 5 | CONCLUSIONS AND RECOMMENDATIONS | 152 |
| 5.1 | Overview | 152 |
| 5.2 | Conclusions | 152 |
| 5.3 | Present Contributions | 154 |
| 5.4 | Limitation | 154 |
| 5.5 | Recommendation | 155 |

| | | |
|-----------------------------|--------------------------------------|-----|
| 5.5.1 | Future Work on Numerical Development | 155 |
| 5.5.2 | Future Work on MHV Simulation | 155 |
| REFERENCES | | 157 |
| APPENDICES | | 180 |
| BIODATA OF STUDENT | | 186 |
| LIST OF PUBLICATIONS | | 187 |



LIST OF TABLES

| Table | Page |
|----------------------------------------------------------------------------------------------------------------------------------------------------------------------------------------------------------------------------------|------|
| 2.1 Previous review of articles complemented by the present study | 10 |
| 2.2 Type of MHVs and their blood clot influences | 12 |
| 2.3 Blood clot factors | 16 |
| 2.4 Estimation of blood clotting model | 18 |
| 2.5 Comparison of different numerical methods for MHV simulation applications | 26 |
| 2.6 Modification of forcing function for pseudo rigid solid treatment | 29 |
| 2.7 Various recent turbulent model uses for MHV and the observation | 38 |
| 2.8 Fixed leaflet MHV simulation | 47 |
| 2.9 Summary of previous MHV numerical studies | 54 |
| 3.1 Coordinate and corresponding α after initialization at interface region $0 < \alpha < 1$ | 72 |
| 3.2 Co_{max} , Co_{α} , α_{max} , α_{min} , and Δt over time | 74 |
| 3.3 Summary of numerical setup used in present works | 84 |
| 3.4 Numerical tests and its objective | 88 |
| 3.5 Centreline velocity and L_2 error for various grid size h and viscosity ratio $\frac{\mu_s}{\mu_f}$ of Poiseuille flow | 92 |
| 3.6 L_2 Errors and convergence rates | 96 |
| 3.7 Numerical error uncertainty analysis based on GCI approach. Variable is at $y/L = 0.24$ | 96 |
| 3.8 Lid-driven flow inside a 2D cavity showing location of the eddies. PE: primary eddy; BR: bottom right; BL: bottom left | 99 |
| 3.9 Grid refinement study for the flow around cylinder with $Re = 40$ | 101 |
| 3.10 Physical parameters of the flow pattern around a circular cylinder at $Re = 40$: Recirculation length L_w/d , separation angle θ_s , location of recirculation centre (a/d , b/d), and Strouhal number St | 102 |
| 3.11 Comparison of L_w and ΔP between present NBF-VOF Cartesian grid method and that of Schafer and Turek (1996) | 106 |
| 3.12 Maximum velocity comparison with different grid resolutions | 111 |
| 4.1 Grid setup for axisymmetric aorta model | 126 |

LIST OF FIGURES

| Figure | Page |
|-----------------------------------------------------------------------------------------------------------------------------------------------------------------------------------------------------------------------------------------------------------------|------|
| 1.1 Similar pattern between postulated (da Vinci's) and measured blood vortices in the aortic root (Source: Bissell et al., 2014) | 2 |
| 1.2 Direction of blood through the valves | 3 |
| 1.3 Schematic view comparison of grid structure between (a) BF, (b) NBF and (c) VOF methods | 5 |
| 2.1 Types of mechanical heart valves: (a) Starr-Edwards caged ball valve; (b) Bjork Shiley tilting disc valve; (c) Medtronic Hall tilting disc valve; and (d) St Jude Medical Regent bileaflet valve (Source: Dangas, 2016) | 11 |
| 2.2 Typical boundary condition for one cycle pulsatile flow showing opening phase (A-B), acceleration phase (B-C), peak flow phase (C-D), deceleration phase (D-E), and closing phase (E-A). Continuous line: Mass flow rate; dash line: Angle of the leaflet | 12 |
| 2.3 (a) Clean MHV; (b) Explanted MHV showing complete immobilization of both leaflets due to blood clot (aortic view); (c) The same explanted MHV (ventricular view) (Source: Tirilomis, 2012) | 13 |
| 2.4 Velocity field of a misaligned valve showing the the flow separation, re-circulation, and shed vortices (Source: Bluestein at al., 2002) | 14 |
| 2.5 Definitions of IB nodes, where the velocities are reconstructed. Filled squares: IB nodes of the fluid with at least one shared solid cell; filled triangles: IB nodes of solid with at least one shared fluid cell (Source: Sotiropoulos and Yang , 2014a) | 21 |
| 2.6 Sketch of the velocity interpolation procedure (Source: Fadlun et al., 2000) | 22 |
| 2.7 Span-wise vorticity on central plane of MHV on pulsatile flow (Source: Yang, 2016) | 23 |
| 2.8 Example of computational grids for the simulation of the flow around a valve placed within a S-shaped duct using (a) IB with cartesian grid, and (b) IB with with a curvilinear grid, so-called CURVIB method (Source: Roman et. al, 2009) | 24 |
| 2.9 Definition of the domain that contains a surface of discontinuity Γ , fluid domain Ω_f , and solid domain Ω_s , in uniform Cartesian grid | 28 |
| 2.10 Schematic shape of the discretized domain (the owner (P) and the neighbour (N) cells) | 32 |
| 2.11 Comparison of 2D vorticity contour at $Re = 5000$ using different RANS models: (a) SA; (b) $k - \epsilon$ (Source: Nguyen et al., 2012) | 39 |
| 2.12 Comparison of velocity profiles for $k - \epsilon$, SA, and LES turbulent model (Source: Kuan et al., 2014) | 39 |
| 2.13 Vorticity structure appearance of two different turbulent models: (a) RANS; (b) hybrid RANS/LES (Source: Ge et al., 2005) | 40 |
| 2.14 Comparison of measured instantaneous out-of-plane vorticity distribution with CFD simulation (Source: Dasi et al., 2007a, Yun et al., 2014) | 42 |

| | | |
|------|-----------------------------------------------------------------------------------------------------------------------------------------------------------------------------------------------------------------------------------------------------------------------------------|----|
| 2.15 | Comparison of velocity profile between experimental measurements of (Ge et al., 2005) and several numerical simulations on MHV for (a) $Re = 6000$, and (b) $Re = 750$ at the cross-sectional location at X_c | 43 |
| 2.16 | Streamlines in the fully-opened phase (Source: Bang et al., 2006) | 44 |
| 2.17 | Computational domain of blood through (a) anatomically realistic aorta (Borazjani et al., 2008), (b) axisymmetric model (Borazjani et al., 2010), and (c) anatomically realistic aorta with LV (Source: Le and Sotiropoulos, 2012) | 45 |
| 2.18 | Comparison of flow field between fixed valve (for steady inflow ($Re = 800$ and 4200) and pulsatile inflow) and moving valve. (a) The shear stress variation at the leading edge of the valve; (b) The transvalvular pressure drop variation (Source: Rosenfeld et al., 2002) | 46 |
| 2.19 | MHV orientations recommended by previous studies relative to the geometry of the aortic root (indicated by lines of valve symmetry through its central orifice), showing left coronary (LC) and right coronary (RC) (Source: Haya, 2015) | 50 |
| 3.1 | Methodology flowchart for NBF-VOF development and their implementation used in present study | 62 |
| 3.2 | Definition of interface boundary with the NBF-VOF Cartesian grid method for (a) 10×10 grid, and (b) 20×20 grid | 67 |
| 3.3 | Lid-driven cavity problem setup for algorithm stability test | 71 |
| 3.4 | The corresponding value of colour function α at cell center at collocated grid. Dash line: exact location of solid-fluid boundary. Empty circle : $\alpha = 0$, filled circle: $\alpha = 1$ | 71 |
| 3.5 | Comparison of colour function α and streamline between original (left panel) and modified $\mathbf{H}(\mathbf{u})$ (right panel) showing different time instant | 73 |
| 3.6 | Comparison of velocity profile between original and modified $\mathbf{H}(\mathbf{u})$ at $y = 0.3$ showing time instant (a) 1 s, (b) 5 s, (c) 8 s, and (d) 10 s. Interface of $\alpha = 0.5$ is at $x = 0.5$ | 75 |
| 3.7 | Comparison of velocity profile between original and modified $\mathbf{H}(\mathbf{u})$ at $y = 0.4$ showing time instant (a) 1 s, (b) 5 s, (c) 8 s, and (d) 10 s. Interface of $\alpha = 0.5$ is at $x = 0.4$ and 0.6 | 76 |
| 3.8 | Comparison of velocity profile between original and modified $\mathbf{H}(\mathbf{u})$ at $y = 0.5$ showing time instant (a) 1 s, (b) 5 s, (c) 8 s, and (d) 10 s. Interface of $\alpha = 0.5$ is at $x = 0.3$ and 0.7 | 77 |
| 3.9 | Spurious oscillation effect due to forcing function shows velocity magnitude versus time at xy coordinate (0.3,0.5) | 78 |
| 3.10 | Setup for lid-driven cavity with embedded domain for differencing test case | 79 |
| 3.11 | Grid used in lid-driven cavity test, with 40×40 for uniform grid | 80 |
| 3.12 | Lid-driven cavity case showing (a) streamline for LUD scheme, and (b) comparison of velocity profile for various schemes at line $y = 0.5$ | 80 |
| 3.13 | Comparison velocity profile for lid-driven cavity test between unstructured, structured grid and with that of Ghia et al. (1982) at line $y = 0.5$ | 81 |

| | | |
|------|------------------------------------------------------------------------------------------------------------------------------------------------------------------------------------------------------------------------------------------------------------------------------------------------------------------|-----|
| 3.14 | Transport of α in lid-driven cavity flow for (a) without interface compression term ($C_a = 0$), and (b) with interface compression term ($C_a = 1$). The initial position of the cylinder is on the black line. The visualized entity is shown for all values of α between 0.01 and 0.99 | 82 |
| 3.15 | Overview of the image-to-computation framework process: (a) Threshold and segmentation image data. Only the interested region is extracted (in this case, the aorta); (b) retained desired domain and map into CFD platform; (c) generate uniform background mesh that covered the selected computational domain | 86 |
| 3.16 | Implementation of OpenFOAM working directory into NBF-VOF method | 87 |
| 3.17 | Configuration of two-dimensional Poiseuille flow. The mesh shown is a coarser grid size of $a/5$ for clear visibility | 90 |
| 3.18 | Poiseuille flow showing (a) comparison of velocity profile between NBF-VOF Cartesian grid method and the theoretical solution (Equation (3.39)), and (b) numerical L_2 error versus the grid distance on different $\frac{\mu_s}{\mu_f}$ constraints | 91 |
| 3.19 | Transient Poiseuille flow using BF and NBF-VOF Cartesian grid methods on different $\frac{\mu_s}{\mu_f}$ constraints | 92 |
| 3.20 | Comparison of computational time between the develop NBF-VOF Cartesian grid method and conventional BF grid methods on Poiseuille flow | 93 |
| 3.21 | Analysis of time step and Co number for transient Poiseuille flow | 93 |
| 3.22 | Lid-driven cavity with embedded solid showing (a) colour function contour on uniform mesh 60×60 (grid size $L/50$), and (b) the resulting velocity streamline | 95 |
| 3.23 | Lid-driven cavity with embedded solid problem showing numerical L_2 error versus the grid distance in logarithmic scale for viscosity ratios 10^3 and 10^6 | 95 |
| 3.24 | Geometrical layout of the flow domain. $\alpha = 0$ is fluid domain, and $\alpha = 1$ is solid domain | 97 |
| 3.25 | Comparison of velocity profile for lid-driven cavity flow at centreline of the cavity between developed NBF-VOF Cartesian grid method and with that of Ghia et al. (1982) showing (a) u_x velocity profile along $x = 0.5$, and (b) u_y velocity profile along $y = 0.5$ | 98 |
| 3.26 | Comparison of streamline pattern for the 2D lid-driven cavity flow at $Re = 1000$ between (a) the developed NBF-VOF Cartesian grid solution, (b) the work of Ghia et al. (1982) | 99 |
| 3.27 | Schematic view of the flow over a cylinder in a free stream with dimension | 100 |
| 3.28 | Zoom view of the NBF-VOF Cartesian grid method on coarse grid at vicinity of cylinder | 100 |
| 3.29 | Time evolution of the recirculation length with three grid sizes | 101 |
| 3.30 | Flow past a circular cylinder showing (a) streamline visualization for $Re = 20$, (b) streamline visualization for $Re = 40$, and (c) parameter definition | 102 |

| | | |
|------|-----------------------------------------------------------------------------------------------------------------------------------------------------------------------------------------------------------------------------------------------------------------------------------------------------------------------------------|-----|
| 3.31 | Flow past a circular cylinder at $Re = 40$ showing a comparison of pressure coefficient C_p between NBF-VOF, BF grid method (Tseng and Ferziger, 2003), and experimental measurements (Grove et al., 1964) | 103 |
| 3.32 | Flow around a cylinder for $Re = 100$ showing (a) the vorticity field, and (b) the vertical velocity versus time for St estimation. The u_y was measured at probe A | 104 |
| 3.33 | Geometry setup with boundary conditions for flow over a cylinder asymmetrically places in a channel | 105 |
| 3.34 | Flow over a cylinder asymmetrically places in a channel showing streamline visualization for (a) $Re = 20$, and (b) $Re = 100$ | 106 |
| 3.35 | Geometry setup for a 90° bend tube flow. The coarse size of NBF grid is shown ($\Delta x = \Delta y = d/8$) | 107 |
| 3.36 | Numerical-experimental comparison of stream wise velocity versus normalise tube diameter 90° tube bend for (a) $\theta = 0^\circ$, (b) $\theta = 23.4^\circ$, (c) $\theta = 58.5^\circ$ and (d) $\theta = 81.9^\circ$, respectively. Normalise distance = 1 for inner curve, and normalise distance = 0 for outer curve | 108 |
| 3.37 | Velocity contour maps: (a) 0° , (b) 22.5° , (c) 45° , (d) 67.5° and (e) 90° , (I: inner curve, O: outer curve). The results presented in the upper half of the figure were derived by De Vosse et al. (1989). Present numerical results are provided in the bottom half | 109 |
| 3.38 | Mesh structure for the (a) BF and (b) NBF-VOF Cartesian grid methods | 110 |
| 3.39 | Grid independency test of velocity profile using at cross-section location $y = -0.188$ for (a) NBF-VOF Cartesian grid and (b) BF grid methods. The corresponding coordinate is shown for (c) NBF-VOF Cartesian grid method, and (d) BF grid method | 112 |
| 3.40 | Velocity contour comparison between the BF and NBF grid methods at eleven cross-section locations during the peak flow instant time. The left bottom subfigure the pulsatile flow impose at the inlet | 113 |
| 3.41 | Velocity contour of u_z at Cross-section B using the (a) NBF-uniform mesh and (b) BF (conventional), (I: inner curve, O: outer curve) | 114 |
| 3.42 | Velocity profile (u_z) at Cross-section B along the line (a) $y = -0.18$; (b) $y = -0.188$, (c) $y = -0.194$, and (d) $y = -0.2$. Refer to Figure 3.39c & d for the respective cross-section location | 116 |
| 3.43 | Comparison of velocity streamline between the BF (a) and NBF-VOF Cartesian grid method (b) shows the helical flow profile in the aorta curvature during the peak flow | 117 |
| 3.44 | Instantaneous vortical structure by the Q-criterion ($Q = 5000$), coloured by velocity magnitude, obtained using newly developed NBF-VOF Cartesian grid and conventional BF grid methods at different instantaneous pulsation time | 118 |
| 4.1 | MHV in axisymmetric aorta flow direction showing the colour function α | 122 |
| 4.2 | MHV in anatomy aorta flow direction showing the colour function α | 122 |
| 4.3 | The flow methodology for MHV simulation analysis. Yellow-filled: Axisymmetric aorta model; blue-filled: Anatomic aorta model | 123 |

| | | |
|------|-------------------------------------------------------------------------------------------------------------------------------------------------------------------------------------------------------------------------------------------------------|-----|
| 4.4 | Pulsatile inflow used in present study for MHV simulation. The analysis concentrate on three instant time namely, accelerating flow (AF) ($t = 0.25$ s), peak flow (PF) ($t = 0.45$ s) and decelerating flow (DF) ($t = 0.45$ s) | 124 |
| 4.5 | Axisymmetric, straight test section. Geometry similar to that used by Dasi et al. (2007) | 125 |
| 4.6 | Numerical geometry of the MHV in axisymmetric aortic root model showing the grid topology | 126 |
| 4.7 | Grid dependency test for axisymmetric aorta at $Re = 750$, $x = 32$ mm. See Figure 4.1 for the plotted line reference | 127 |
| 4.8 | Segmented images aorta from CT scan | 128 |
| 4.9 | Combination of tube and anatomic sinus | 128 |
| 4.10 | Numerical geometry of the MHV in anatomy aorta showing the grid topology | 129 |
| 4.11 | Grid dependency test for anatomic aorta at $Re = 750$, $x = 45$ mm. See Figure 4.2 for the plotted line reference | 130 |
| 4.12 | Experimental-numerical comparison for steady flow at $Re = 750$, for (a) near leaflet tips ($x = 32$ mm), (b) middle of sinus ($x = 48$ mm), and (c) end of sinus ($x = 61$ mm). See Figure 4.1 for the plotted line reference | 131 |
| 4.13 | Experimental-numerical comparison for steady flow at $Re = 6000$, for (a) near leaflet tips ($x = 32$ mm), (b) middle of sinus ($x = 48$ mm), and (c) end of sinus ($x = 61$ mm). See Figure 4.1 for the plotted line reference | 132 |
| 4.14 | Comparison of 2D vorticity between present NBF-VOF Cartesian grid method, previous simulation (Yun et al., 2014b) and experiments measurement (Yun et al., 2014b) during PF phases | 133 |
| 4.15 | Comparison of vorticity contour using different turbulence models: (a) SA (Nguyen et al., 2012); (b) $k - \epsilon$ (Nguyen et al., 2012); (c) URANS (Ge et al., 2005); (d) DES (Ge et al., 2005); and (e) LES, present NBF-VOF Cartesian grid method | 134 |
| 4.16 | Velocity magnitude at the central xy plane for (a) anatomic, AF, (b) axisymmetric, AF, (c) anatomic, PF, (d) axisymmetric, PF, (e) Anatomic, DF, and (f) axisymmetric, DF | 136 |
| 4.17 | Velocity vector at the central xy plane during PF for (a) axisymmetric aorta case and (b) anatomic aorta case | 137 |
| 4.18 | Streamline pattern at the central xy plane during PF for (a) anatomic and (b) axisymmetric aorta. The point source of the streamline is taken at the tip of the leaflet with radius 0.005 | 138 |
| 4.19 | Streamline pattern for anatomic model during (a) AF (b) PF and (c) DF | 139 |
| 4.20 | 2D vorticity contour at the central xy plane for (a) anatomic, AF, (b) axisymmetric, AF, (c) anatomic, PF, (d) axisymmetric, PF, (e) anatomic, DF, and (f) axisymmetric, DF | 140 |
| 4.21 | Instantaneous vortical structures visualised by iso-surfaces of $\lambda_2 a = -10000$ for an anatomic aorta | 142 |
| 4.22 | TKE contour at time instant PA for (a) anatomic, xy plane, (b) anatomic, xz plane, (c) axisymmetric, xy plane, and (d) axisymmetric, xz plane | 143 |

| | | |
|------|-------------------------------------------------------------------------------------------------------------------------------------------------------------------------------------------------------------------------------------------------------------------------------------------------------------------------------------------|-----|
| 4.23 | Viscous stress contour at the central xy plane for (a) anatomic, AF, (b) axisymmetric, AF, (c) anatomic, PF; (d) axisymmetric, PF, (e) anatomic, DF, and (f) Axisymmetric, DF. With contour scaling capped at $\tau_{eq} = 10$ Pa. | 145 |
| 4.24 | Viscous stress contour at xz plane during PF for (a) bottom leaflet (b) top leaflet, and (c) between leaflets | 146 |
| 4.25 | Viscous stress contour at yz plane during PF at (a) trailing, (b) middle, and (c) leading edge of leaflet | 147 |
| 4.26 | Comparison of viscous stresses profile at vicinity area of leading edge of the leaflet for a complete cardiac cycle | 147 |
| 4.27 | Comparison of viscous stresses profile at the central xy plane for (a) anatomic, leaflet tip, $x = 45$ mm, (b) anatomic, sinus middle, $x = 55$ mm, (c) anatomic, end of sinus, $x = 63$ mm, (d) axisymmetric, leaflet tip at $x = 32$ mm, (e) axisymmetric, sinus middle, $x = 48$ mm, and (f) Axisymmetric, end of sinus, $x = 61$ mm | 149 |
| 4.28 | Seeded particle for corresponding flow time showing particle age in seconds | 150 |
| B.1 | Anatomic geometry of aorta with valve showing (a) front view (y plane) (b) top view (z plane) and (c) side view (x plane) | 185 |
| B.2 | Modeled geometry of aorta with valve showing (a)side view, (b) front view, and (c) top view | 185 |

LIST OF ABBREVIATIONS

| | |
|----------------|---------------------------------------------------------------|
| AF | accelerating flow |
| ALE | arbitrary lagrangian eulerian |
| ATS | american thoracic society |
| avg | average |
| BD | blended bifferencing |
| BDI | blood damage index |
| BF | boundary fitted |
| BHV | bioprosthetic heart valve |
| BMHV | bileaflet mechanical heart valve |
| CD | central differencing |
| CFD | computational fluid dynamics |
| CPU | central processing unit |
| CT | computed tomography |
| CURVIB | curvilinear immersed boundary method |
| CVD | cardiovascular diseases |
| DES | detached eddy simulation |
| DF | decelerating flow |
| DFG | Deutsche Forschungsgemeinschaft (German Research Association) |
| DNS | direct numerical simulation |
| EFD | experimental fluid dynamics |
| FCT | flux corrected transport |
| FD | fictitious domain |
| F _s | safety factor |
| FVM | finite volume method |
| GCI | grid convergence index |
| IB | immersed boundary |
| IIM | immersed interface method |
| IJN | Institut Jantung Negara (National Health Institute) |
| IMM | immersed membrane method |
| LBM | lattice boltzman method |
| LC | left coronary |
| LES | large eddy simulation |
| LUD | Linear upwind differencing |
| LV | left ventricle |
| MHV | mechanical heart valve |
| MPI | message passing interface |
| MRI | magnetic resonance imaging |
| MULES | Multi-dimensionals limiter for explicit solution |
| NBF | non-boundary fitted |
| NBF-VOF | non-boundary fitted/volume of fluid |
| PCG | preconditioned conjugate gradient |
| PDEs | partial differential equations |

| | |
|-------|-----------------------------------------|
| PF | peak flow |
| PIV | particle image velocimetry |
| PLIC | piecewise linear interface construction |
| RANS | reynolds average navier stokes |
| RBC | red blood cell |
| RC | right coronary |
| RSS | reynolds shear stress |
| SA | spalart almaras |
| SGS | sub-grid scale |
| sim | simulation |
| SJM | st jude medical |
| SLIC | simple line interface calculation |
| SPH | smooth particle hydrodynamics |
| SST | shear stress transport |
| TSS | turbulent shear stress |
| TVD | total variation diminishing |
| URANS | unsteady reynolds average navier stokes |
| UD | upwind differencing |
| VS | vortical structural |
| VOF | volume of fluid |
| w | width |
| WSS | wall shear stress |
| XFEM | extended finite element method |

Symbol

| | |
|----------------------------|--------------------------------------------------------------------------|
| a | matrix coefficient |
| a, b | recirculation length location for the flow around cylinder |
| $[A]$ | squared matrix of the coefficients |
| C | model constants for BDI |
| Co | courant number |
| Co_{α} | interface courant number |
| C_k, C_e | turbulent coefficient for LES |
| C_p | pressure coefficient |
| C_u | turbulent variable dependent on the rate of deformation and spin tensors |
| d | diameter |
| \mathbf{f} | forcing function |
| F | flux |
| \overline{fN} | distance between center of cell P and face center of cell P |
| G | elasticity coefficient |
| h | grid size |
| H | height |
| $\mathbf{H}(\mathbf{U})$ | original off-diagonal matrices coefficient |
| $\mathbf{H}(\mathbf{U})^*$ | modified off-diagonal matrices coefficient |
| I_{red} | reduced moment of inertia |
| K | dean number |
| k_{SGS} | turbulent kinetic energy |
| L_w | recirculation length |

| | |
|-----------------|------------------------------------------------------------------------------------------------------------|
| L_2 | error norm |
| \mathbf{n} | normal direction |
| \mathbf{n}_f | normal vector of the cell surface |
| N | total number of grid |
| P | pressure |
| p | order of accuracy |
| P_∞ | free stream Pressure |
| \overline{PN} | distance between center of cell P and center of cell N |
| Q | second tensor invariant |
| $[R]$ | source term vector |
| r | smoothness monitor or r-factor for TVD differencing schemes or grid refinement ratio |
| Re | reynolds number |
| R_c | radius of curvature for bend |
| S | deformation rate (strain-rate) tensor or surface area vector or symmetric part of the velocity gradient |
| St | strouhal number |
| S_p | linear part of the source term |
| S_u | constant part of the source term |
| S_ϕ | source term |
| t | time |
| \mathbf{u} | velocity vector |
| u | velocity magnitude |
| \mathbf{u}_c | relative velocity |
| V | volume |
| ω | vorticity |
| (x_a, y_a) | coordinate at front of cylinder |
| (x_e, y_e) | coordinate at end of cylinder |

Greek

| | |
|------------------------|------------------------------------------------------|
| α | VOF color function |
| α_{\max} | maximum value of color function |
| α_{\min} | minimum value of color function |
| Γ | interface or difusivity |
| γ | forcing function constant |
| δ | curvature ratio of the tube bend |
| Δ | difference |
| Δt | time step size |
| Δt_{\max} | max time step |
| ε | turbulent energy dissipation, Penalization parameter |
| ζ | damping coefficient |
| η | forcing function constant |
| θ | angle or leaflet's angle |
| θ_s | separation angle |
| κ | Interface curvature or bulk viscosity |
| λ | lagrange multiplier or tensor eigenvalue |
| λ_2 | second invariant of tensor |
| λ_1, λ_2 | adaptive time step coefficient |

| | |
|-------------|----------------------------------------------|
| μ | dynamic viscosity |
| μ_f | fluid dynamic viscosity |
| μ_s | solid dynamic viscosity |
| μ_t | turbulent dynamic viscosity |
| μ_{SGS} | eddy viscosity |
| ν | kinematic viscosity |
| ρ | density |
| σ | surface tension |
| τ | shear stress or period of vortex shedding |
| τ_w | wall shear stress |
| τ_{eq} | equivalent shear stress |
| τ_e | stress tensor for hyperelastic material |
| ϕ | general scalar property |
| ξ | moment around the hinge axis |
| Ω | antisymmetric parts of the velocity gradient |
| Ω_f | Continuous of fluid domain |
| Ω_s | embedded or solid domain |
| ψ | TVD limiter |
| Ω_1 | continuous domain properties |
| Ω_2 | embedded domain properties |

Superscripts

| | |
|--------------|--------------------------------|
| , | fluctuating component |
| T | transpose |
| α | model constants for BDI |
| β | model constants for BDI |
| n | discrete time level |
| L | linear term for the flux F |
| NL | non-linear term for the flux F |
| $\bar{\phi}$ | filtered variable |

Subscripts

| | |
|---------|--------------------------|
| (i,j) | (x,y) cell coordinates |
| x,y,z | coordinate components |
| f | face interpolation |
| N | neighbouring cell N |
| P | owner cell P |
| SGS | turbulent SGS properties |

CHAPTER 1

INTRODUCTION

1.1 Motivation

Imagine that a person has accidentally cut his finger. After some time, the blood will begin to clot to stop the finger from bleeding. That is the good function of blood clotting. However, if a blood clot develops in a patient's heart valve due to some abnormal flow, there is a possibility that the clot may break off and go to the brain (causing a stroke) or to other organs in the body. In certain cases, the blood could clot at the valve itself and cause it to malfunction. To avoid this, blood thinners (usually warfarin) must be taken at the right dosage everyday with periodic blood tests and dietary restrictions (Cannegieter et al., 1994; Shoeb and Fang, 2013). This routine may change the lifestyle of the patient. A second complication is bleeding due to the use of blood thinners. A patient taking a blood thinner may encounter a problem when he is injured or requires surgery, whereby during the surgery, the use of the blood thinner has to be controlled to prevent excessive bleeding during the operation. This puts the patient at risk. It has been reported that the risk of both bleeding and blood clots is 1-2% each year. Therefore, for a patient who receives an artificial heart valve at the age of 40 years and lives to the age of 80 years, there is a 40-80% chance of both bleeding and blood clotting occurring (Shoeb and Fang, 2013). Moreover, the use of blood thinners will also cause birth mortality among young women who wish to have children (Vitale et al., 1999; Neumann et al., 2016).

Scientific knowledge of the heart dates back as far as the beginnings of recorded history. Among the first people to investigate and write about the anatomy of the heart was the Greek physician, Erasistratus (around 250 BC), and Claudius Galenus (around 129-201) who was a Greek-born Roman physician. Later, Leonardo da Vinci (1452-1519) also made some advances in the understanding of blood flow (Gharib et al., 2002). Briefly, da Vinci believed that the valve was closed during a forward flow by the vortex that forms behind the valve leaflets through his drawing in Figure 1.1. Nevertheless, after nearly 500 years later, finding an accurate quantitative description of the cardiac function still poses a challenge. Only just recently, in 2014, da Vinci's vortex formation and re-circulation were reported in-vivo (Bissell et al., 2014) and in-vitro (Querzoli et al., 2014) studies and direct comparison have been made.



Figure 1.1: Similar pattern between postulated (da Vinci's) and measured blood vortices in the aortic root
(Source: Bissell et al., 2014)

Cardiovascular disease (CVD) remains the leading global cause of death, accounting for more than 17.3 million deaths per year in 2013 worldwide, according to the American Heart Association's 2017 Heart Disease and Stroke Statistics Update (Benjamin et al., 2017). It represents 31 % of all global deaths, a number that is expected to grow to more than 23.6 million by 2030. More than 75% of CVD deaths occur in low-income and middle-income countries, and 80% of all CVD deaths are due to heart attacks and strokes.

One of the CVD is associated with the malfunction of heart valves such as stenosis (heart valve that does not open properly) and regurgitation (backflow of blood as the valves are closing). Figure 1.2 shows the flow direction of blood through the valves. Unrepaired valves necessitate surgery so that the artificial heart valves replacement can be done. It is estimated that more than 300,000 replacement heart valves are implanted annually worldwide (Jahandardoost et al., 2016). Since the first implantation of artificial heart valves in 1952, significant risks, such as the need for anticoagulation drugs and re-surgery operation, are still present. Current artificial heart valves suffer from several problems such as blood cell damage (haemolysis) and formation of the blood clot (thrombosis) (Yoganathan et al., 2004; Borazjani, 2015; Bark et al., 2016). This complication requires patients to undergo anticoagulant therapy, which may lead to life-threatening haemorrhage or stroke if poorly managed.

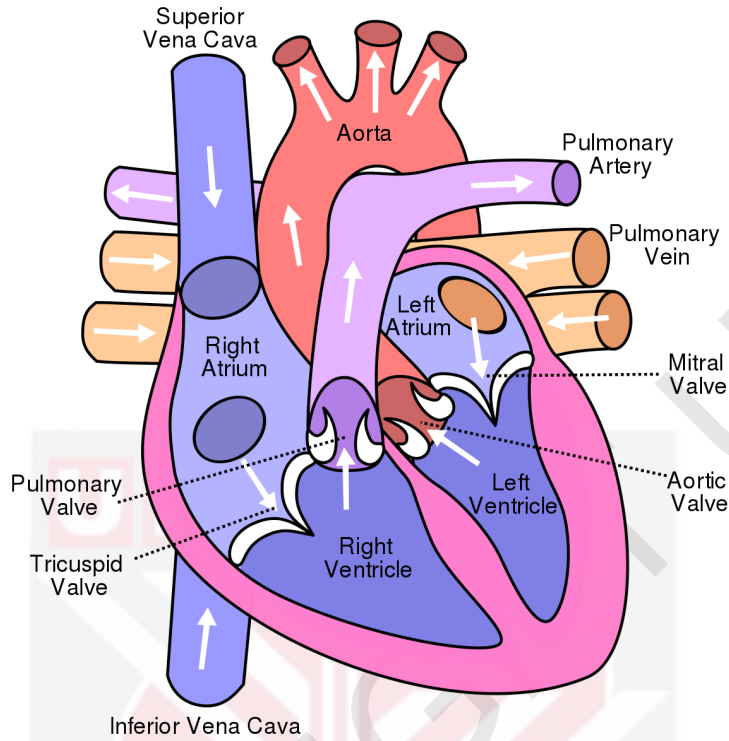


Figure 1.2: Direction of blood through the valves

1.2 Computational Modelling of Cardiovascular Flow

A thorough understanding of the aerodynamic characteristics in blood flow is needed to improved artificial heart valve performance. Although the measurement of aerodynamic properties through current advance medical imaging devices are feasible, such as magnetic resonance imaging (MRI), computed tomography (CT) scans, and echocardiography (Mittal et al., 2016), it remains to be a complicated process for determining the local influence of fluid mechanical factors such as viscous stress on the blood constituents (Yokoi et al., 2005). Furthermore, experimental work in this focus area is expensive and limited. Alternatively, using mathematical equations through a numerical method and simulation should be adopted.

Being able to look into the heart through mathematical equations would be a fantastic achievement. The visualisation of the blood flow behaviours in the heart, for example through the heart valve has become an interest in the computational fluid dynamics (CFD) community for the last few decades due to the increasing use of supercomputer nowadays.

CFD simulations can provide valuable information to the medical device manufacturers and surgeons in making critical decisions in the treatment of heart valve repair or replacements. The visualisation will enable them to access the level of disease (such as blood clotting) in great detail. Whether either CFD information will allow access to the level of disease in great detail or not, it will continue to be the subject of intense debate in literature (Yun et al., 2014a; Jahandardoost et al., 2016).

Nevertheless, CFD modelling is widely used to unravel many engineering problems, for example, in the design and manufacturing of aircrafts (Ahmad et al., 2005; Firdaus et al., 2016; Ismail and Roe, 2009; Aftab et al., 2016), marine technology (Carrica et al., 2013; Zakaria et al., 2013), electronic cooling (Abdullah et al., 2009), and recently in the biomedical field (Riazuddin et al., 2010; Zakaria et al., 2016; Basri et al., 2016). Many of these engineering problems involve complex geometries that do not fit exactly in Cartesian co-ordinates (Versteeg and Malalasekera, 2007). When the flow boundary does not coincide with the co-ordinate lines of a cartesian grid, one could proceed by non-Cartesian grid coordinate systems (i.e. cylindrical, axisymmetric three-dimensional or spherical co-ordinates). For the worst cases, randomized, skewed and distorted grid may be used.

Grid generation represents a critical step in modelling complex geometry and is usually performed using unstructured meshing algorithms conforming to the surface geometry which leads to poor mesh generation. The poor mesh in turn will influence the accuracy, stability and convergence of the numerical solution. Although hexahedral Cartesian meshes are known to provide a higher accuracy and reduce the computational costs, their application in computational cardiovascular studies is challenging due to the complex and branching topology of vascular territories. Due to this restraint, the use of accurate CFD simulations in the medical field is still sparse in literature, and its numerical development continues to be of major interest in research.

There are two main types of grid meshes for complex geometry: boundary fitted (BF) methods and non-boundary-fitted (NBF) methods. BF volume mesh is created around the imported geometry. The BF method will usually generate a poor unstructured tetrahedral mesh quality. Poor quality surface and volume meshes can result in difficulties with the solution of the flow problem, ranging from inaccurate solutions to non-convergence of the solution process. Therefore, to generate a high-quality mesh, significant user effort is usually required to perform the meshing procedure at the boundary when the boundary-fitted (BF) grid method is used. This task is an additional burden and is tedious. With the NBF method, the underlying grid does not coincide with the geometry of the surface being treated, thus efficiently generating the Cartesian hexahedral mesh.

The earlier study of fluid flow using the NBF method in the biomedical field was done by Peskin (1977), where the so-called immersed boundary (IB) method was introduced to simulate the fluid flow problem in a heart valve. Later, further improvements to the method were developed such as the fictitious domain method (Glowinski et al., 1999; Yu et al., 2013), cut cell method (Meinke et al., 2013; Qin and Krivodonova, 2013), and

ghost fluid method (Fedkiw et al., 1999; Liu, 2014), just to name a few. These methods use local forcing function to identify a solid object, which comes with several issues such as unaligned between boundary and grid, blur interface, and stiffness of the governing equations. Another method is volume of fluid (VOF) (Hirt and Nichols, 1981; Takagi et al., 2012) mostly used to solve multiphase fluid flow problem. In VOF method, colour function α is used to distinguish between fluid and solid, where $\alpha = 1$ is solid, and $\alpha = 0$ is fluid. The implementation VOF method for fluid-solid geometry is sparse but rarely can be found in literature such as in (Ravoux et al., 2003; Ng, 2009). A schematic view comparison between the traditional BF, common NBF and VOF methods representation grid is shown in Figure 1.3.

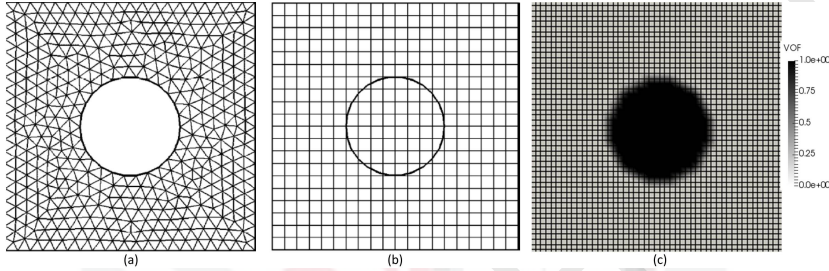


Figure 1.3: Schematic view comparison of grid structure between (a) BF, (b) NBF and (c) VOF methods

In this work, a robust procedure of new NBF method combining with VOF method without the local forcing function was proposed. The methodology adopted in this work is designed so that it could be suitably implemented in an open source code, OpenFOAM, and could be used to solve fluid flow problems in the biomedical field faced by scientists and researchers. Such a numerical study may not require substantial changes to existing CFD codes, particularly those codes done in-house by specific researchers. Furthermore, medical imaging techniques provide the multi-component geometry as voxel data for each patient, which would share the same ground as the Cartesian grid VOF colour function. As far as the authors know, present work is the first to implement an NBF grid technique through a simple extension of the VOF interface capturing scheme, particularly for MHV flow in blood clotting estimation.

1.3 Problem Statement

The MHV is prone to blood clotting. A blood clot can be estimated from the accumulation of the shear stress and residence time of the platelet. For the Newtonian fluid, the shear stress was proportional to the velocity gradient. The velocity gradient can yield the complex flow such as vorticity, stagnation flow, and separation. To be able to capture this rich dynamic complex flow structure in pulsation and highly turbulent flow, high order accurate numerical methods are needed to discretising and solving the governing equations numerically.

The numerical accuracy and stability are mainly influenced by the mesh quality. For a simple 2D test case on uniform Cartesian grids, a second-order method should remain close to the second-order accuracy. However, when the grids are uniformly distorted (skewed), a second-order finite volume method (FVM) can drop to less than the second-order (Ismail et al., 2010; Chizari and Ismail, 2015). Furthermore, in randomised grids, a second-order FVM can behave very erratically (negative order of accuracy) (Chizari and Ismail, 2016). The meshing for complex geometry using conventional BF method is always either unstructured, high aspect ratio, high skewness, or non-orthogonal. These characteristics affect the accuracy and stability of the numerical method. To ensure uniform Cartesian grid used for the whole computational domain regardless the complexity of the geometry, non-boundary-fitted (NBF) grid method is a perfect candidate.

However, previous NBF grid method faced several issues. Firstly, the grid point did not necessarily coincide with the boundary node (Fadlun et al., 2000); making interpolating the velocity is necessary. Secondly, the resolution at the interface is smeared in a few grid cells, thus required very fine mesh at the interface. Finally, the forcing function in previous NBF method required a user-defined parameter. This parameter must be chosen in as such a way that to balance between producing solid nature of embedded domain and to avoid numerical oscillation, at a reasonable computational cost. Too large forcing function parameter will increase the stiffness of the governing equations and, therefore, affect convergence properties (Engels et al., 2015).

Therefore, this study intends to fill the gap of knowledge to develop a new NBF method for a pseudo-rigid-body, using the idea of mixture properties of viscosity μ and colour function α of the volume of fluid (VOF). As no additional forcing function is needed, the new method hypothesises that the global user defines parameters that do not affect the overall accuracy, convergence and total computational cost. The newly developed method will be demonstrated for the first time with real MHV flow implant in the aorta to see the potential of blood clotting. It is hypothesised that the developed method is feasible for modelling the blood flow in through MHV in the aorta.

1.4 Research Objectives

The ultimate goal of this research is to develop a new fluid flow numerical method using NBF grid method on the Cartesian grid for the flow on a complex stationary domain. The method must be able to integrate medical images and accurately simulate the flow field through the heart valves, showing the non-physiological flow patterns, responsible for blood clotting. To achieve this objective, the focus of the thesis will be on the following specific aims:

1. To identify issues and current research direction on numerical method, and aerody-

namics characteristics on blood clot potential for MHV simulation.

2. To develop a new Cartesian NBF grid method for complex geometry namely, non-boundary-fitted/volume of fluid (NBF-VOF) Cartesian grid method.
3. To validate a new develop NBF-VOF Cartesian grid method with conventional BF method, previous NBF method, and previous experimental result using a series of benchmark tests.
4. To verify the develop NBF-VOF Cartesian grid method in simulating blood flow through the MHV located in an axisymmetric and anatomic aorta to access the flow pattern and location of blood clot potential.

1.5 Scopes of the Studies

The present study was bounded by the following scopes,

1. This study involved numerical works, where a new mathematical method was introduced and integrated with Opensource OpenFOAM CFD platform via editable C++ code. Nevertheless, to validate the solver, comparison with available numerical and experimental data was made. For MHV, existing experimental work in literature was used for validation purposes.
2. The turbulent model available in the literature varied, ranging from RANS, LES and DNS. In this study, only one model was used, which was the LES turbulent model, since a previous study (Nguyen et al., 2012) reported it could handle rich dynamic flow field in MHV. Furthermore, LES is more superior than common RANS model because it can solve instantaneous details of flow field, which is required in blood clot formation simulation (Anupindi et al., 2013; Yun et al., 2014b). Therefore, investigating or implementation of any other turbulent model is currently beyond the scope of the study.
3. Among the variety of MHV available in the market for clinical practice, present study used the St Jude Mechanical (SJM) heart valve model as the computational model. This type has good hemodynamic flow and covers over 80% implanted into the patient (Mirkhani et al., 2016). It has plenty of numerical and experimental data solution. Furthermore, many researchers use them as a model for CFD code validation purpose (i.e. (Yun et al., 2014b; Jahandardoost et al., 2016)).
4. The leaflet was treat stationary which is sufficient to access the blood clot potential. Therefore, present study developed a method that was suitable for fixed boundaries only, and the fixed valve's leaflet was chosen instead.
5. The blood properties were assumed to be Newtonian since the size of the heart and surrounding blood vessels was larger by at least three orders of magnitude than

the typical blood cell (the typical size of blood cells is of the order of $10\ \mu\text{m}$). Therefore, when considering flow phenomena associated with heart valves, it is treated blood, for the most part, as a continuum medium that was incompressible and Newtonian (Sotiropoulos et al., 2016). Therefore discussion up to molecular level is also beyond the scope of the study.

1.6 Thesis Outline

This thesis is divided into five chapters including an introductory chapter (Chapter 1). Followed by Chapter 2, where present study provided the comprehensive literature review concerning numerical methodologies for the solution of the BF and NBF method, method for estimating blood clotting, experimental cases suitable for the heart valve validation, and some parametric study that contribute to blood clotting.

Furthermore, Chapter 3 is the primary framework of this thesis where the gap was illustrated. The mathematical formulation and solution strategy for the modified NBF method, namely NBF-VOF grid method is shown. This chapter also show the bridging between previous old method to present new method. Two treatments were made: 1) impose high viscous solid and 2) modification of the linear system of Navier-Stokes equations. In Chapter 3, a comprehensive validation and verification was also done. The validation data was taken from analytical solution, established existing numerical and experimental data. Furthermore, the new method also validated using conventional BF method with real aorta vessel as test geometry.

Moreover, Chapter 4 discusses the application or practical contribution of current NBF-VOF method in a real complex geometry of medical image data. Although the validation of the solver is extensively done in Chapter 3, present study continue to provide the model validation using asymmetric aorta case, where an experimental and numerical solution exists. Present study also compared the flow field between the axisymmetric and anatomic aorta and accessed the potential of blood clot potential.

Finally, the conclusion of the entire finding is done in Chapter 5 together with a recommendation for future work. It is also worth to mention that some content of this thesis has been published in journal articles and the list of publication is presented in the appropriate section.

REFERENCES

- AbdelMigid, T. A., Saqr, K. M., Kotb, M. A., and Aboelfarag, A. A. (2017). Revisiting the lid-driven cavity flow problem: Review and new steady state benchmarking results using GPU accelerated code. *Alexandria Engineering Journal*, 56(1):123–135.
- Abdullah, M. K., Abdullah, M. Z., Ramana, M. V., Khor, C. Y., Ahmad, K. A., Mujeebu, M. A., Ooi, Y., and Ripin, Z. M. (2009). Numerical and experimental investigations on effect of fan height on the performance of piezoelectric fan in microelectronic cooling. *International Communications in Heat and Mass Transfer*, 36(1):51–58.
- Aftab, S. M. A., Razak, N. A., Ra, A. S. M., and Ahmad, K. A. (2016). Progress in Aerospace Sciences Mimicking the humpback whale : An aerodynamic perspective. *Progress in Aerospace Sciences*, 84:48–69.
- Ahmad, K. A., Mcewan, W. T., Watterson, J. K., and Cole, J. S. (2005). Numerical Study of a vibrating sub-boundary layer vortex generator. In *35th AIAA Fluid Dynamics Conference and Exhibit*, pages 1–9, Toronto, Ontario Canada. AIAA.
- Akutsu, T., Matsumoto, A., and Takahashi, K. (2011). In Vitro Study of the Correlation between the Aortic Flow Field Affected by the Bileaflet Mechanical Valves and Coronary Circulation. In *5th European Conference of the International Federation for Medical and Biological Engineering*, pages 769–772. Springer.
- Alauzet, F., Fabrèges, B., Fernández, M. A., and Landajuela, M. (2016). Nitsche-XFEM for the coupling of an incompressible fluid with immersed thin-walled structures. *Computer Methods in Applied Mechanics and Engineering*, 301:300–335.
- Albadawi, A., Donoghue, D., Robinson, A., Murray, D., and Delauré, Y. (2013). Influence of surface tension implementation in Volume of Fluid and coupled Volume of Fluid with Level Set methods for bubble growth and detachment. *International Journal of Multiphase Flow*, 53:11–28.
- Alemu, Y. and Bluestein, D. (2007). Flow-induced platelet activation and damage accumulation in a mechanical heart valve: Numerical studies. *Artificial Organs*, 31(9):677–688.
- Aliabadi, A. (2013). *Numerical simulation of fluid-structure interaction for tilting-disk mechanical heart valves*. PhD thesis.
- Anderson, J. D. and Wendt, J. (1995). *Computational fluid dynamics*, volume 206. Springer.
- Angot, P., henri Bruneau, C., and Fabrie, P. (1999). Numerische Mathematik A penalization method to take into account obstacles in incompressible viscous flows. *Numerische Mathematik*, 81(4):497–520.
- Annerel, S., Claessens, T., Degroote, J., Segers, P., and Vierendeels, J. (2014a). Validation of a numerical FSI simulation of an aortic BMHV by in vitro PIV experiments. *Medical engineering & physics*, 36(8):1014–23.

- Annerel, S., Claessens, T., Taelman, L., Degroote, J., Van Nooten, G., Verdonck, P., Segers, P., and Vierendeels, J. (2014b). Influence of Valve Size, Orientation and Downstream Geometry of an Aortic BMHV on Leaflet Motion and Clinically Used Valve Performance Parameters. *Annals of Biomedical Engineering*, 43(6):1370–1384.
- Annerel, S., Degroote, J., Claessens, T., Dahl, S. K., Skallerud, B., Hellevik, L. R., Van Ransbeeck, P., Segers, P., Verdonck, P., and Vierendeels, J. (2012). A fast strong coupling algorithm for the partitioned fluidstructure interaction simulation of BMHVs. *Computer Methods in Biomechanics and Biomedical Engineering*, 15(12):1281–1312.
- Anupindi, K., Delorme, Y., Shetty, D. A., and Frankel, S. H. (2013). A novel multiblock immersed boundary method for large eddy simulation of complex arterial hemodynamics. *Journal of Computational Physics*, 254:200–218.
- Apel, J., Paul, R., Klaus, S., Siess, T., and Reul, H. (2001). Assessment of Hemolysis Related Quantities in a Microaxial Blood Pump by Computational Fluid Dynamics. *Artificial Organs*, 25(5):341–347.
- Appanaboyina S, F. M., Lohner, R., Putman C M, and R, C. J. (2008). Computational fluid dynamics of stented intracranial aneurysms using adaptive embedded unstructured grids. *International Journal for Numerical Methods in Fluids*, 57:475–493.
- Astorino, M., Gerbeau, J. F., Pantz, O., and Traoré, K. F. (2009). Fluid-structure interaction and multi-body contact: Application to aortic valves. *Computer Methods in Applied Mechanics and Engineering*, 198(45-46):3603–3612.
- Azwadi, N., Shukri, Z. M., and Afiq Witri, M. Y. (2012). Numerical investigation of 2D lid driven cavity using smoothed particle hydrodynamics (SPH) method. In *American Institute of Physics Conference Series*, volume 1440, pages 789–798.
- Balaras, E. (2004). Modeling complex boundaries using an external force field on fixed Cartesian grids in large-eddy simulations. *Computers and Fluids*, 33(3):375–404.
- Bang, J. S., Yoo, S. M., and Kim, C. N. (2006). Characteristics of pulsatile blood flow through the curved bileaflet mechanical heart valve installed in two different types of blood vessels: velocity and pressure of blood flow. *ASAIO Journal*, 52(3):234–242.
- Bark, D. L., Vahabi, H., Bui, H., Movafaghi, S., Moore, B., Kota, A. K., Popat, K., and Dasi, L. P. (2016). Hemodynamic Performance and Thrombogenic Properties of a Superhydrophobic Bileaflet Mechanical Heart Valve. *Annals of Biomedical Engineering*, pages 1–12.
- Barker, A. J., Markl, M., Bürk, J., Lorenz, R., Bock, J., Bauer, S., Schulz-menger, J., and Knobelsdorff-brenkenhoff, F. V. (2012). Bicuspid Aortic Valve Is Associated With Altered Wall Shear Stress in the Ascending Aorta. *Circulation: Cardiovascular Imaging*, 5(4):457–466.
- Basri, A. A., Zuber, M., Zakaria, M. S., Basri, E. I., Aziz, A. F. A., Ali, R. M., Tamagawa, M., and Ahmad, K. A. (2016). The Hemodynamic Effects of Paravalvular Leakage Using Fluid Structure Interaction; Transcatheter Aortic Valve Implantation Patient. *Journal of Medical Imaging and Health Informatics*, 6(6):1513–1518.

- Bavo, A. M., Rocatello, G., Iannaccone, F., Degroote, J., Vierendeels, J., and Segers, P. (2016). Fluid-Structure Interaction Simulation of Prosthetic Aortic Valves: Comparison between Immersed Boundary and Arbitrary Lagrangian-Eulerian Techniques for the Mesh Representation. *Plos One*, 11(4):1–17.
- Benjamin, E. J., Blaha, M. J., Chiuve, S. E., Cushman, M., Das, S. R., Deo, R., de Ferranti, S. D., Floyd, J., Fornage, M., , and others Gillespie, C. (2017). Heart disease and stroke statistics 2017 update. *Circulation*, 135(10):e146–e603.
- Berberovic, E., Hinsberg, N. P. V., Jakirli, S., Roisman, I. V., and Tropea, C. (2009). Drop impact onto a liquid layer of finite thickness : Dynamics of the cavity evolution. *Physical Review E*, 79(3):036306.
- Biasetti, J., Hussain, F., and Gasser, T. C. (2011). Blood flow and coherent vortices in the normal and aneurysmatic aortas : a fluid dynamical approach to intra- luminal thrombus formation. *Journal of The Royal Society Interface*, 8:1449–1461.
- Bissell, M. M., Dall’Armellina, E., and Choudhury, R. P. (2014). Flow vortices in the aortic root: In vivo 4D-MRI confirms predictions of Leonardo da Vinci. *European Heart Journal*, 35(20):1344.
- Black, M. M. and Drury, P. J. (1994). Mechanical and other problems of artificial valves. In *The Pathology of Devices*, pages 127–159. Springer.
- Bluestein, D., Gutierrez, C., Londono, M., and Schoepfoerster, R. T. (1999). Vortex Shedding in Steady Flow Through a Model of an Arterial Stenosis and Its Relevance to Mural Platelet Deposition. *Annals of biomedical engineering*, 27(6):763–773.
- Bluestein, D., Li, Y. M., and Krukenkamp, I. B. (2002). Free emboli formation in the wake of bi-leaflet mechanical heart valves and the effects of implantation techniques. *Journal of Biomechanics*, 35:1533–1540.
- Bluestein, D., Rambod, E., and Gharib, M. (2000). Vortex Shedding as a Mechanism for Free Emboli Formation in Mechanical Heart Valves. *Journal of Biomechanical Engineering*, 122:125–134.
- Bonet, J. and Wood, R. D. (2008). *Nonlinear Continuum Mechanics for Finite Element Analysis*. Cambridge University Press, Cambridge.
- Bonomi, D., Vergara, C., Faggiano, E., Stevanella, M., Conti, C., Redaelli, A., Puppini, G., Faggian, G., Formaggia, L., and Luciani, G. B. (2015). Influence of the aortic valve leaflets on the fluid-dynamics in aorta in presence of a normally functioning bicuspid valve. *Biomechanics and Modeling in Mechanobiology*, 14(16):1349–1361.
- Borazjani, I. (2013). Fluidstructure interaction, immersed boundary-finite element method simulations of bio-prosthetic heart valves. *Computer Methods in Applied Mechanics and Engineering*, 257:103–116.
- Borazjani, I. (2015). A Review of Fluid-Structure Interaction Simulations of Prosthetic Heart Valves. 25:75–93.

- Borazjani, I., Ge, L., Le, T., and Sotiropoulos, F. (2013). A parallel overset-curvilinear-immersed boundary framework for simulating complex 3D incompressible flows. *Computers & fluids*, 77:76–96.
- Borazjani, I., Ge, L., and Sotiropoulos, F. (2008). Curvilinear immersed boundary method for simulating fluid structure interaction with complex 3D rigid bodies. *Journal of Computational Physics*, 227(16):7587–7620.
- Borazjani, I., Ge, L., and Sotiropoulos, F. (2010). High-Resolution FluidStructure Interaction Simulations of Flow Through a Bi-Leaflet Mechanical Heart Valve in an Anatomic Aorta. *Annals of Biomedical Engineering*, 38(2):326–344.
- Borazjani, I. and Sotiropoulos, F. (2010). The effect of implantation orientation of a bileaflet mechanical heart valve on kinematics and hemodynamics in an anatomic aorta. *Journal of biomechanical engineering*, 132(11):111005.
- Boris, J. P. and Book, D. L. (1973). Flux-corrected transport. I. SHASTA, a fluid transport algorithm that works. *Journal of Computational Physics*, 11(1):38–69.
- Bovendeerd, P. H. M., Steenhoven, A. A. V., Vosse, F. N. V. D., and Vossers, G. (1987). Steady entry flow in a curved pipe. *Journal of Fluid Mechanics*, 177:233–246.
- Caltagirone, J.-P. and Vincent, S. (2001). Sur une methode de penalisation tensorielle pour la resolution des equations de Navier-Stokes. *Comptes Rendus de l'Academie des Sciences-Series IIB-Mechanics*, 329(8):607–613.
- Cannegieter, S. C., Rosendaal, F. R., and Briet, E. (1994). Thromboembolic and bleeding complications in patients with mechanical heart valve prostheses. *Circulation*, 89(2):635–641.
- Carey, R. F., Porter, J. M., Richard, G., Luck, C., Shu, M. C., Guo, G. X., Elizondo, D. R., Kingsbury, C., Anderson, S., and Herman, B. A. (1995). An interlaboratory comparison of the FDA protocol for the evaluation of cavitation potential of mechanical heart valves. *The Journal of heart valve disease*, 4(5):532–539.
- Carrica, P. M., Ismail, F., Hyman, M., Bhushan, S., and Stern, F. (2013). Turn and zigzag maneuvers of a surface combatant using a URANS approach with dynamic overset grids. *Journal of marine science and technology*, 18(2):166–181.
- Celik, I. B., Ghia, U., Roache, P. J., and Others (2008). Procedure for estimation and reporting of uncertainty due to discretization in CFD applications. *Journal of fluids Engineering-Transactions of the ASME*, 130(7).
- Chandra, S., Rajamannan, N. M., and Sucosky, P. (2012). Computational assessment of bicuspid aortic valve wall-shear stress: implications for calcific aortic valve disease. *Biomechanics and Modeling in Mechanobiology*, 11:1085–1096.
- Chandran, K. B. (1992). *Cardiovascular biomechanics*. New York University Press, University of California.

- Chandran, K. B. (2010). Role of Computational Simulations in Heart Valve Dynamics and Design of Valvular Prostheses. *Cardiovascular engineering and technology*, 1(1):18–38.
- Chandran, K. B. and Aluri, S. (1997). Mechanical Valve Closing Dynamics : Relationship between Velocity of Closing , Pressure Transients , and Cavitation Initiation. *Annals of biomedical engineering*, 25(6):926–938.
- Chandran, K. B., Dexter, E. U., Aluri, S., and Richenbacher, W. E. (1998). Negative pressure transients with mechanical heart-valve closure: correlation between in vitro and in vivo results. *Annals of biomedical engineering*, 26(4):546–556.
- Chang, G.-z. D. (1970). Numerical solutions for steady flow past a circular cylinder at Reynolds numbers up to 100. *J. Fluid Mech.*, 42:471–489.
- Cheng, R., Lai, Y. G., and Chandran, K. B. (2003). Two-dimensional fluid-structure interaction simulation of bileaflet mechanical heart valve flow dynamics. *The Journal of heart valve disease*, 12(6):772–780.
- Cheng, R., Lai, Y. G., and Chandran, K. B. (2004). Three-dimensional Fluid-Structural Interaction Simulation of Bileaflet Mechanical Heart Valve Flow Dynamics. *Annals of Biomedical Engineering*, 32(11):1471–1483.
- Chizari, H. and Ismail, F. (2015). Accuracy Variations in Residual Distribution and Finite Volume Methods on Triangular Grids. *Bulletin of the Malaysian Mathematical Sciences Society*, pages 1–34.
- Chizari, H. and Ismail, F. (2016). A Grid-Insensitive LDA Method on Triangular Grids Solving the System of Euler Equations. *Journal of Scientific Computing*, pages 1–36.
- Choi, C. R. and Kim, C. N. (2009). Numerical analysis on the hemodynamics and leaflet dynamics in a bileaflet mechanical heart valve using a fluid-structure interaction method. *ASAIO Journal*, 55(5):428–37.
- Choi, C. R., Kim, C. N., Kwon, Y. J., and Lee, J. W. (2003). Pulsatile blood flows through a bileaflet mechanical heart valve with different approach methods of numerical analysis; pulsatile flows with fixed leaflets and interacted with moving leaflets. *KSME International Journal*, 17(7):1073–1082.
- Chung, M.-h. (2006). Cartesian cut cell approach for simulating incompressible flows with rigid bodies of arbitrary shape. *Computers & Fluids*, 35:607–623.
- Collins, F. and Collins, F. (2014). Effect of Hypertension on the Closing Dynamics and Lagrangian Blood Damage Index Measure of the B-Datum Regurgitant Jet in a Bileaflet Mechanical Heart Valve. *Annals of Biomedical Engineering*, 42(1):110–122.
- Corbett, S. C., Ajdari, A., Coskun, A. U., and Nayeb-Hashemi, H. (2010). Effect of pulsatile blood flow on thrombosis potential with a step wall transition. *ASAIO journal*, 56(4):290–295.

- Coutanceau, Madeleine and Bouard, R. (1977). Experimental determination of the main features of the viscous flow in the wake of a circular cylinder in uniform translation. Part 1. Steady flow. *Journal of Fluid Mechanics*, 79(2):231–256.
- Damián, S. M. (2013). *An Extended Mixture Model for the Simultaneous Treatment of Short and Long Scale Interfaces*. PhD thesis, Universidad Nacional del Litoral.
- Damian, S. M. and Norberto M. Nigro (2014). An extended mixture model for the simultaneous treatment of small-scale and large-scale interfaces. *International Journal for Numerical Methods in Fluids*, (75):547–574.
- Dangas, G. D., Weitz, J. I., Giustino, G., Makkar, R., and Mehran, R. (2016). Prosthetic Heart Valve Thrombosis. *Journal of the American College of Cardiology*, 68(24):2670–2689.
- Dasi, L. P., Ge, L., Simon, A. H., Sotiropoulos, F., and Yoganathan, P. A. (2007). Vorticity dynamics of a bileaflet mechanical heart valve in an axisymmetric aorta. *Physics of Fluids*, 19(6).
- De Hart, J., Baaijens, F. P. T., Peters, G. W. M., and Schreurs, P. J. G. (2003a). A computational fluid-structure interaction analysis of a fiber-reinforced stentless aortic valve. *Journal of Biomechanics*, 36:699–712.
- De Hart, J., Peters, G. W., Schreurs, P. J., and Baaijens, F. P. (2000). A two-dimensional fluid-structure interaction model of the aortic valve [correction of value]. *Journal of biomechanics*, 33:1079–1088.
- De Hart, J., Peters, G. W. M., Schreurs, P. J. G., and Baaijens, F. P. T. (2003b). A three-dimensional computational analysis of fluid-structure interaction in the aortic valve. *Journal of Biomechanics*, 36:103–112.
- De Hart, J., Peters, G. W. M., Schreurs, P. J. G., and Baaijens, F. P. T. (2004). Collagen fibers reduce stresses and stabilize motion of aortic valve leaflets during systole. *Journal of Biomechanics*, 37(3):303–311.
- De Tullio, M. D., Afferrante, L., Demelio, G., Pascasio, G., and Verzicco, R. (2011a). Fluid-structure interaction of deformable aortic prostheses with a bileaflet mechanical valve. *Journal of biomechanics*, 44(9):1684–1690.
- De Tullio, M. D., Cristallo, A., Balaras, E., Verzicco, R., David, V. R., and Vergata, T. (2009). Direct numerical simulation of the pulsatile flow through an aortic bileaflet mechanical heart valve. *Journal of Fluid Mechanics*, 622:259.
- De Tullio, M. D., Pascasio, G., Weltert, L., De Paulis, R., and Verzicco, R. (2011b). Evaluation of prosthetic-valved devices by means of numerical simulations. *Philosophical transactions. Series A, Mathematical, physical, and engineering sciences*, 369(1945):2502–2509.
- De Tullio, M. D., Pedrizzetti, G., and Verzicco, R. (2011c). On the effect of aortic root geometry on the coronary entry-flow after a bileaflet mechanical heart valve implant: A numerical study. *Acta Mechanica*, 216(1-4):147–163.

- De Vosse, F. N., Van Steenhoven, A. A., Segal, A., and Janssen, J. D. (1989). A finite element analysis of the steady laminar entrance flow in a 90 degree curved tube. *International Journal For Numerical Methods in Engineering*, 9:275–287.
- DeVilliers, E. (2006). *The Potential of Large Eddy Simulation for the Modeling of Wall Bounded Flows*. PhD thesis.
- Dillard, S. I., Mousel, J. A., Shrestha, L., Raghavan, M. L., and Vigmostad, S. C. (2014). From medical images to flow computations without user-generated meshes. *International Journal for Numerical Methods in Biomedical Engineering*, 30:1057–1083.
- Donea, J., Giuliani, S., and Halleux, J. (1982). An arbitrary lagrangian-eulerian finite element method for transient dynamic fluid-structure interactions. *Computer Methods in Applied Mechanics and Engineering*, 33:689–723.
- Dumont, K., Stijnen, J. M. a., Vierendeels, J., van de Vosse, F. N., and Verdonck, P. R. (2004). Validation of a fluid-structure interaction model of a heart valve using the dynamic mesh method in fluent. *Computer methods in biomechanics and biomedical engineering*, 7(3):139–146.
- Dumont, K., Vierendeels, J., Kaminsky, R., van Nooten, G., Verdonck, P., and Bluestein, D. (2007). Comparison of the hemodynamic and thrombogenic performance of two bileaflet mechanical heart valves using a CFD/FSI model. *Journal of biomechanical engineering*, 129(4):558–565.
- Einav, S. and Bluestein, D. (2004). Dynamics of blood flow and platelet transport in pathological vessels. *Annals of the New York Academy of Sciences*, 1015(1):351–366.
- Engels, T., Kolomenskiy, D., Schneider, K., and Sesterhenn, J. (2015). Numerical simulation of fluidstructure interaction with the volume penalization method. *Journal of Computational Physics*, 281:96–115.
- Esmailzadeh, H. and Passandideh-Fard, M. (2014). Numerical and Experimental Analysis of the Fluid-Structure Interaction in Presence of a Hyperelastic Body. *Journal of Fluids Engineering*, 136(11):111107.
- Fadlun, E., Verzicco, R., Orlandi, P., and Mohd-Yusof, J. (2000). Combined immersed-boundary finite-difference methods for three-dimensional complex flow simulations. *Journal of Computational Physics*, 161(1):35–60.
- Faggiano, E., Antiga, L., Puppini, G., Quarteroni, A., Luciani, G. B., and Vergara, C. (2013). Helical flows and asymmetry of blood jet in dilated ascending aorta with normally functioning bicuspid valve. *Biomechanics and Modeling in Mechanobiology*, 12(4):801–813.
- Fallon, A. M., Dasi, L. P., Marzec, U. M., Hanson, S. R., and Yoganathan, A. P. (2008). Procoagulant Properties of Flow Fields in Stenotic and Expansive Orifices. *Annals of Biomedical Engineering*, 36(1):1–13.
- Fedkiw, R., Aslam, T., Merriman, B., and Osher, S. (1999). A Non-oscillatory Eulerian Approach to Interfaces in Multimaterial Flows (the Ghost Fluid Method). *Journal of Computational Physics*, 152(2):457–492.

- Ferziger, J. H. and Peric, M. (2002). *Computational Methods for Fluid Dynamics*. Springer, Berlin Heidelberg New York, third edition.
- Figliola, R. S. and Mueller, T. J. (1981). On the Hemolytic and Thrombogenic Potential of Occluder Prosthetic Heart Valves From In-Vitro Measurements. *Journal of Biomechanical Engineering*, 103(2):83–90.
- Firdaus, M. A., Shahrine, A. M., Yusoff, H., and Arifin, K. A. (2016). Flapping wing micro-aerial-vehicle : kinematics , membranes , and flapping mechanisms of or-nithopter and insect flight. *Chinese Journal of Aeronautics*, 29(5):1159–1177.
- Forsythe, N. and Mueller, J.-D. (2007). Validation of a fluidstructure interaction model for a bileaflet mechanical heart valve. *International Journal of Computational Fluid Dynamics*, 22(8):541–553.
- Freudenberger, R. S., Hellkamp, A. S., Halperin, J. L., Poole, J., Anderson, J., Johnson, G., Mark, D. B., Lee, K. L., and Bardy, G. H. (2007). Risk of Thromboembolism in Heart Failure : An Analysis From the Sudden Cardiac Death in Heart Failure Trial (SCD-HeFT). *Circulation*, 115(20):2637–2641.
- Fureby, C., Gosman, A. D., Tabor, G., Weller, H. G., Sandham, N., and Wolfshtein, M. (1997). Large eddy simulation of turbulent channel flows. *Turbulent shear flows*, 11:13–28.
- Ge, L., Dasi, L. P., Sotiropoulos, F., and Yoganathan, A. P. (2008). Characterization of hemodynamic forces induced by mechanical heart valves: Reynolds vs. viscous stresses. *Annals of Biomedical Engineering*, 36(2):276–297.
- Ge, L., Jones, S. C., Sotiropoulos, F., Healy, T. M., and Yoganathan, A. P. (2003). Numerical simulation of flow in mechanical heart valves: grid resolution and the assumption of flow symmetry. *Journal of biomechanical engineering*, 125(5):709–718.
- Ge, L., Leo, H. L., Fotis, S., and Yoganathan, A. (2005). Flow in a mechanical bileaflet heart valve at laminar and near-peak systole flow rates: CFD simulations and experiments. *Journal of biomechanical engineering*, 127(5):782–797.
- Ge, L. and Sotiropoulos, F. (2007). A numerical method for solving the 3D unsteady incompressible Navier-Stokes equations in curvilinear domains with complex immersed boundaries. *Journal of Computational Physics*, 225(2):1782–1809.
- Gharib, M., Kremers, D., Koochesfahani, M. M., and Kemp, M. (2002). Leonardo ’ s vision of flow visualization. *Experiments in Fluids*, 33(1):219–223.
- Ghia, U., Ghia, K., and Shin, C. (1982). High-Re solutions for incompressible flow using the Navier-Stokes equations and a multigrid method. *Journal of Computational Physics*, 48:387–411.
- Gilmanov, A., Le, T. B., and Sotiropoulos, F. (2015). A numerical approach for simulating fluid structure interaction of flexible thin shells undergoing arbitrarily large deformations in complex domains. *Journal of Computational Physics*, 300:814–843.

- Gilmanov, A. and Sotiropoulos, F. (2005). A hybrid Cartesian/immersed boundary method for simulating flows with 3D, geometrically complex, moving bodies. *Journal of Computational Physics*, 207(2):457–492.
- Gilmanov, A., Sotiropoulos, F., and Balaras, E. (2003). A general reconstruction algorithm for simulating flows with complex 3D immersed boundaries on Cartesian grids. *Journal of Computational Physics*, 191(2):660–669.
- Glowinski, R., Pan, T. W., Hesla, T. I., and Joseph, D. D. (1999). A distributed Lagrange multiplier/fictitious domain method for particulate flows. *International Journal of Multiphase Flow*, 25(5):755–794.
- Goldstein, D., Handler, R., and Sirovich, L. (1993). Modeling a no-slip flow boundary with an external force field. *Journal of Computational Physics*, 305(2):354–366.
- Griffith, B. E. (2011). Immersed boundary model of aortic heart valve dynamics with physiological driving and loading conditions. *International Journal for Numerical Methods in Biomedical Engineering*, 28(1):1–29.
- Griffith, B. E., Hornung, R. D., McQueen, D. M., and Peskin, C. S. (2007). An adaptive, formally second order accurate version of the immersed boundary method. *Journal of Computational Physics*, 223(1):10–49.
- Griffith, B. E., Luo, X., M., M. D., and Peskin, C. S. (2009). Simulating the Fluid Dynamics of Natural and Prosthetic Heart Valves Using the Immersed Boundary Method. *International Journal of Applied Mechanics*, 01(01):137–177.
- Grigioni, M., Daniele, C., Avenio, G. D., and Barbaro, V. (2001). The influence of the leaflets' curvature on the flow field in two bileaflet prosthetic heart valves. *Journal of Biomechanics*, 34(5):613–621.
- Grigioni, M., Daniele, C., Del Gaudio, C., Morbiducci, U., Balducci, A., Davenio, G., and Barbaro, V. (2005a). Three-Dimensional Numeric Simulation of Flow Through an Aortic Bileaflet Valve in a Realistic Model of Aortic Root. *ASAIO Journal*, 51(3):176–183.
- Grigioni, M., Morbiducci, U., Avenio, G. D., Di, G., Costantino, B., and Gaudio, D. (2005b). A novel formulation for blood trauma prediction by a modified power-law mathematical model. *Biomechanics and Modeling in Mechanobiology*, 4(4):249–260.
- Gross, J. M., Guo, G. X., and Hwang, N. H. (1990). Venturi pressure cannot cause cavitation in mechanical heart valve prostheses. *ASAIO transactions/American Society for Artificial Internal Organs*, 37(3):M357–8.
- Gross, J. M., Shermer, C. D., and Hwang, N. H. C. (1988). Vortex shedding in bileaflet heart valve prostheses. *ASAIO Journal*, 34(3):845–850.
- Grove, A. S., Shair, F. H., Petersen, E. E., and Acrivos, A. (1964). An experimental investigation of the steady separated flow past a circular cylinder. *Journal of Fluid Mechanics*, 19(1964):60–80.

- Gueyffier, D., Li, J., Nadim, A., Scardovelli, R., and Zaleski, S. (1999). Volume-of-Fluid Interface Tracking with Smoothed Surface Stress Methods for Three-Dimensional Flows. *Journal of Computational Physics*, 152:423–456.
- Guivier, C., Deplano, V., and Pibarot, P. (2007). New insights into the assessment of the prosthetic valve performance in the presence of subaortic stenosis through a fluid-structure interaction model. *Journal of Biomechanics*, 40(10):2283–2290.
- Guivier-Curien, C., Deplano, V., and Bertrand, E. (2009). Validation of a numerical 3-D fluid-structure interaction model for a prosthetic valve based on experimental PIV measurements. *Medical engineering & physics*, 31(8):986–993.
- Haeri, S. and Shrimpton, J. S. (2012). On the application of immersed boundary, fictitious domain and body-conformal mesh methods to many particle multiphase flows. *International Journal of Multiphase Flow*, 40:38–55.
- Halevi, R., Hamdan, A., Marom, G., Lavon, K., Ben-Zekry, S., Raanani, E., Bluestein, D., and Haj-Ali, R. (2016). Fluid–structure interaction modeling of calcific aortic valve disease using patient-specific three-dimensional calcification scans. *Medical & biological engineering & computing*, 54(11):1683–1694.
- Hansbo, A. and Hansbo, P. (2002). An unfitted finite element method , based on Nitsche’s method , for elliptic interface problems. *Computer Methods in Applied Mechanics and Engineering*, 191:5537–5552.
- Hart, J. D. (2002). Fluid-Structure Interaction in the Aortic Heart Valve a three-dimensional computational analysis. *Thesis*.
- Hart, J. D., Peters, G. W. M., Schreurs, P. J. G., and Baaijens, F. P. T. (2003). A three-dimensional computational analysis of fluid structure interaction in the aortic valve. *Journal of Biomechanics*, 36:103–112.
- Hasenkam, J. M., Ringgaard, S., Houliind, K., Botnar, R. M., St dkilde Jorgensen, H., Boesiger, P., and Pedersen, E. M. (1999). Prosthetic heart valve evaluation by magnetic resonance imaging q. *European journal of cardio-thoracic surgery*, 16(3):300–305.
- Hashimoto, S., Manabe, S., Matsumoto, Y., Ikegami, K., and Tsuji, H. (2000). The Effect of Pulsatile Shear Flow on Thrombus Formation and Hemolysis. In *22nd Annual EMBS International Conference*, pages 2461–2462, Chicago.
- He, Z., Xi, B., Zhu, K., and Hwang, N. H. (2001). Mechanisms of mechanical heart valve cavitation: investigation using a tilting disk valve model. *The Journal of heart valve disease*, 10(5):666–674.
- Hellums, J. D., Peterson, D. M., Stathopoulos, N. A., Moake, J. L., and Giorgio, T. D. (1987). Studies on the mechanisms of shear-induced platelet activation. In *Cerebral ischemia and hemorheology*, pages 80–89. Springer.
- Hirt, C. and Nichols, B. (1981). Volume of fluid (VOF) method for the dynamics of free boundaries. *Journal of Computational Physics*, 39:201–225.

- Hong, T. and Kim, C. N. (2011). A numerical analysis of the blood flow around the Bileaflet Mechanical Heart Valves with different rotational implantation angles. *Journal of Hydrodynamics, Ser. B*, 23(5):607–614.
- Horgue, P., Prat, M., and Quintard, M. (2014). A penalization technique applied to the "Volume-Of-Fluid" method: Wettability condition on immersed boundaries. *Computers and Fluids*, 100:255–266.
- Hose, D. R., Narracott, A. J., Penrose, J. M. T., Baguley, D., Jones, I. P., and Lawford, P. V. (2006). Fundamental mechanics of aortic heart valve closure. *Journal of biomechanics*, 39(5):958–967.
- Huang, Z. J. and Merkle, C. L. (1994). Numerical simulation of unsteady laminar flow through a tilting disk heart valve: prediction of vortex shedding. *Journal of Biomechanics*, 11(4):391–402.
- Hunt, J. C. R., Wray, A. A., and Moin, P. (1989). Eddies, streams, and convergence zones in turbulent flows. *Proceedings of the Summer Program 1988*, (1970):193–208.
- Hutchison, C., Sullivan, P., and Ethier, C. R. (2011). Measurements of steady flow through a bileaflet mechanical heart valve using stereoscopic PIV. *Medical & biological engineering & computing*, 49:325–335.
- Hwang, N. H. (1998). Cavitation potential of pyrolytic carbon heart valve prostheses: a review and current status. *The Journal of heart valve disease*, 7(2):140.
- Iaccarino, G., Verzicco, R., Bari, P., and David, V. R. (2003). Immersed boundary technique for turbulent flow simulations. *Applied Mechanics Reviews*, 56(3):331.
- Ikeno, T. and Kajishima, T. (2007). Finite-difference immersed boundary method consistent with wall conditions for incompressible turbulent flow simulations. *Journal of Computational Physics*, 226:1485–1508.
- Ismail, F., Carrica, P. M., Xing, T., and Stern, F. (2010). Evaluation of linear and nonlinear convection schemes on multidimensional non-orthogonal grids with applications to KVLCC2 tanker. *International Journal for Numerical Methods in Fluids*, 64:850–886.
- Ismail, F. and Roe, P. L. (2009). Affordable, entropy-consistent Euler flux functions II: Entropy production at shocks. *Journal of Computational Physics*, 228(15):5410–5436.
- Jahandardoost, M., Fradet, G., and Mohammadi, H. (2016). Effect of Pulsatility Rate on the Hemodynamics of Bileaflet Mechanical Prosthetic Heart Valves (St. Jude Medical valve) for the Aortic Position in the Opening Phase; A Computational Study. *Proceedings of the Institution of Mechanical Engineers, Part H: Journal of Engineering in Medicine*, 230:1–16.
- Jeong, J. and Hussain, F. (1995). On the identification of a vortex. *Journal of fluid mechanics*, 285:69–94.
- Jesty, J., Yin, W., Perrotta, P., and Bluestein, D. (2003). Platelet activation in a circulating flow loop: combined effects of shear stress and exposure time. *Platelets*, 14(3):143–149.

- J.U Brackbill, D.B Kothe, C. Z. (1992). A continuum method for modeling surface tension. *Journal of Computational Physics*, 100:335–354.
- Kafesjian, R., Howanec, M., Ward, G., Diep, L., Wagstaff, L., and Rhee, R. (1994). Cavitation damage of pyrolytic carbon in mechanical heart valves. *The Journal of heart valve disease*, 3:2–7.
- Kamensky, D., Hsu, M.-C., Schillinger, D., Evans, J. a., Aggarwal, A., Bazilevs, Y., Sacks, M. S., and Hughes, T. J. R. (2015). An immersogeometric variational framework for fluid-structure interaction: application to bioprosthetic heart valves. *Computer methods in applied mechanics and engineering*, 284:1005–1053.
- Khadra, K., Angot, P., Parneix, S., and Caltagirone, J.-p. (2000). Fictitious domain approach for numerical modelling of Navier Stokes equations. *International Journal for Numerical Methods in Fluids*, 34:651–684.
- Khalafvand, S. S., Ng, E. Y. K., Zhong, L., and Hung, T. K. (2012). Fluid-dynamics modelling of the human left ventricle with dynamic mesh for normal and myocardial infarction : Preliminary study. 42:863–870.
- Kilner, P. J., Yang, G. Z., and Mohiaddin, R. H. (1993). Helical and Retrograde Secondary Flow Patterns in the Aortic Arch Studied by Three-Directional Magnetic Resonance Velocity Mapping. *Circulation*, 88(5):2235–2247.
- King, M. J., Corden, J., David, T., and Fisher, J. (1996). A three-dimensional, time-dependent analysis of flow through a bileaflet mechanical heart valve: Comparison of experimental and numerical results. *Journal of Biomechanics*, 29(5):609–618.
- Kirkpatrick, M. P., Armfield, S. W., and Kent, J. H. (2003). A representation of curved boundaries for the solution of the Navier-Stokes equations on a staggered three-dimensional Cartesian grid. *Journal of Computational Physics*, 184(1):1–36.
- Kleine, P., Hasenkam, M. J., Nygaard, H., Perthel, M., Wesemeyer, D., and Laas, J. (2000). Tilting disc versus bileaflet aortic valve substitutes: intraoperative and post-operative hemodynamic performance in humans. *The Journal of heart valve disease*, 9(2):308–311.
- Kleine, P., Perthel, M., Nygaard, H., Hansen, S. B., Paulsen, P. K., Riis, C., and Laas, J. (1998). Medtronic Hall versus St. Jude Medical mechanical aortic valve: downstream turbulences with respect to rotation in pigs. *The Journal of heart valve disease*, 7(5):548–555.
- Kleine, P., Scherer, M., Abdel-Rahman, U., Klesius, A. A., Ackermann, H., and Moritz, A. (2002). Effect of mechanical aortic valve orientation on coronary artery flow: comparison of tilting disc versus bileaflet prostheses in pigs. *The Journal of thoracic and cardiovascular surgery*, 124(5):925–932.
- Kodama, H., Takeshita, K., and Araki, T. (2004). Fluid particle dynamics simulation of charged colloidal suspensions. *Journal of physics: condensed matter*, 115(16):115–123.

- Krafczyk, M., Cerrolaza, M., Schulz, M., and Rank, E. (1998). Analysis of 3D transient blood flow passing through an artificial aortic valve by Lattice Boltzmann methods. *Journal of Biomechanics*, 31:453–462.
- Krafczyk, M., Tolke, J., Rank, E., and Schulz, M. (2001). Two-dimensional simulation of uid structure interaction using lattice-Boltzmann methods. *Computer and Structures*, 79:2031–2037.
- Krishnan, S., Udaykumar, H. S., Marshall, J. S., and Chandran, K. B. (2006). Two-dimensional dynamic simulation of platelet activation during mechanical heart valve closure. *Annals of Biomedical Engineering*, 34(10):1519–1534.
- Kuan, Y. H., Kabinejadian, F., Nguyen, V.-t., Su, B., Yoganathan, A. P., and Leo, H. L. (2014). Computer Methods in Biomechanics and Biomedical Engineering Comparison of hinge microflow fields of bileaflet mechanical heart valves implanted in different sinus shape and downstream geometry. *Computer Methods in Biomechanics and Biomedical Engineering*, 18(16):37–41.
- Kunkelmann, C. and Stephan, P. (2010). Modification and Extension of a Standard Volume of Fluid Solver For Simulating Boiling Heat Transfer. In *V European Conference on Computational Fluid Dynamics*, number June, pages 14–17.
- Lai, Y. G., Chandran, K. B., and Lemmon, J. (2002). A numerical simulation of mechanical heart valve closure fluid dynamics. *Journal of Biomechanics*, 35:881–892.
- Lakshmi P Dasi, Simon, H. A., Sucusky, P., Yoganathan, A. P., Dasi, L. P., Simon, H. A., Sucusky, P., and Yoganathan, A. P. (2009). Fluid mechanics of artificial heart valves. *Clinical and experimental pharmacology & physiology*, 36(2):225–237.
- Le, T. B. and Sotiropoulos, F. (2012). Fluidstructure interaction of an aortic heart valve prosthesis driven by an animated anatomic left ventricle. *Journal of Computational Physics*, 244:41–62.
- Lee, C. S. and Chandran, K. B. (1995). Numerical simulation of instantaneous back-flow through central clearance of bileaflet mechanical heart valves at closure: shear stress and pressure fields within clearance. *Medical and Biological Engineering and Computing*, 33(3):257–263.
- Leo, H. L. (2005). *An In Vitro Investigation of the Flow Fields Through Bileaflet and Polymeric Prosthetic Heart Valves*. PhD thesis, Georgia Institute of Technology.
- Leonard, A. (1985). Computing three-dimensional incompressible flows with vortex elements. *Annual Review of Fluid Mechanics*, 17(1):523–559.
- Li, C.-P. and Lu, P.-C. (2012). Numerical comparison of the closing dynamics of a new trileaflet and a bileaflet mechanical aortic heart valve. *Journal of artificial organs : the official journal of the Japanese Society for Artificial Organs*, 15(4):364–74.
- Li, C.-P., Lu, P.-C., Liu, J.-S., Lo, C.-W., and Hwang, N. H. (2008). Role of vortices in cavitation formation in the flow across a mechanical heart valve. *The Journal of heart valve disease*, 17(4):435–445.

- Linick, M. and Fasel, H. (2005). A high-order immersed interface method for simulating unsteady incompressible flows on irregular domains. *Journal of Computational Physics*, 204:157–192.
- Liu, C. (2014). *A Cartesian Grid Method for Free Surface Flow Interaction with Complex Geometry*. PhD thesis, Kyushu University.
- Liu, J. S., Lu, P. C., and Chu, S. H. (2000). Turbulence Characteristics Downstream of Bileaflet Aortic Valve Prostheses. *Journal of biomechanical engineering*, 122(2):118–124.
- Löhner, R., Cezbral, J. R., Camelli, F. E., Appanaboyina, S., Baum, J. D., Mestreau, E. L., and Soto, O. A. (2008). Adaptive embedded and immersed unstructured grid techniques. *Computer Methods in Applied Mechanics and Engineering*, 197(25-28):2173–2197.
- Lu, P.-C., Liu, J.-S., Huang, R.-H., Lo, C.-W., Lai, H.-C., and Hwang, N. H. (2004). The Closing Behavior of Mechanical Aortic Heart. *ASAIO journal*, 50(4):294–300.
- Luo, H., Dai, H., Ferreira de Sousa, P. J., and Yin, B. (2012). On the numerical oscillation of the direct-forcing immersed-boundary method for moving boundaries. *Computers & Fluids*, 56:61–76.
- Marom, G. (2014). Numerical Methods for Fluid-Structure Interaction Models of Aortic Valves. *Archives of Computational Methods in Engineering*, 22(4):595–620.
- Marom, G., Haj-Ali, R., Raanani, E., Schäfers, H.-J., and Rosenfeld, M. (2012). A fluid-structure interaction model of the aortic valve with coaptation and compliant aortic root. *Medical & Biological Engineering & Computing*, 50(2):173–182.
- Marom, G., Kim, H. S., Rosenfeld, M., Raanani, E., and Haj-Ali, R. (2013). Fully coupled fluid-structure interaction model of congenital bicuspid aortic valves: Effect of asymmetry on hemodynamics. *Medical and Biological Engineering and Computing*, 51:839–848.
- Massing, A., Larson, M. G., and Logg, A. (2013). Efficient Implementation of Finite Element Methods on Nonmatching and Overlapping Meshes in Three Dimensions. *SIAM Journal on Scientific Computing*, 35(1):c23–c47.
- Meinke, M., Schneiders, L., Günther, C., and Schröder, W. (2013). A cut-cell method for sharp moving boundaries in Cartesian grids. *Computers & Fluids*, 85:135–142.
- Miljoen, H., Herck, P. V., Paelinck, B., Colli, A., Ducci, A., and Burriesci, G. (2016). Possible Subclinical Leaflet Thrombosis in Bioprosthetic Aortic Valves. *The New England Journal of Medicine*, 374(16):1590–1592.
- Mirkhani, N., Davoudi, M. R., Hanafizadeh, P., Javidi, D., and Saffarian, N. (2016). On-X Heart Valve Prosthesis: Numerical Simulation of Hemodynamic Performance in Accelerating Systole. *Cardiovascular Engineering and Technology*, 7(3).
- Mirzaii, I. and Passandideh-Fard, M. (2012). Modeling free surface flows in presence of an arbitrary moving object. *International Journal of Multiphase Flow*, 39:216–226.

- Mittal, R., Hee, J., Vedula, V., Choi, Y. J., Liu, H., Huang, H. H., Jain, S., Younes, L., Abraham, T., and George, R. T. (2016). Computational modeling of cardiac hemodynamics : Current status and future outlook. *Journal of Computational Physics*, 305:1065–1082.
- Mittal, R. and Iaccarino, G. (2005). Immersed Boundary Methods. *Annual Review of Fluid Mechanics*, 37(1):239–261.
- Mohammadi, H., Ahmadian, M. T., and Wan, W. K. (2006). Time-dependent analysis of leaflets in mechanical aortic bileaflet heart valves in closing phase using the finite strip method. *Medical Engineering & Physics*, 28:122–133.
- Mohammadi, H. and Mequanint, K. (2011). Prosthetic aortic heart valves: Modeling and design. *Medical Engineering and Physics*, 33(2):131–147.
- Mohd-Yusof, J. (1997). Combined immersed-boundary/B-spline methods for simulations of flow in complex geometries. *Annual Research Briefs. NASA Ames Research Center*, pages 317–327.
- Morbiducci, U., Ponzini, R., Nobili, M., Massai, D., Montecocchi, F. M., Bluestein, D., and Redaelli, A. (2009). Blood damage safety of prosthetic heart valves. Shear-induced platelet activation and local flow dynamics: A fluid-structure interaction approach. *Journal of Biomechanics*, 42:1952–1960.
- Morsi, Y. S., Yang, W. W., Wong, C. S., and Das, S. (2007). Transient fluid-structure coupling for simulation of a trileaflet heart valve using weak coupling. *Journal of artificial organs : the official journal of the Japanese Society for Artificial Organs*, 10(2):96–103.
- Mousel, J. A. (2012). *A massively parallel adaptive sharp interface solver with application to mechanical heart valve simulations*. PhD thesis, University of Iowa.
- Murphy, D. W., Dasi, L. P., Vukasinovic, J., Glezer, A., and Yoganathan, A. P. (2010). Reduction of procoagulant potential of b-datum leakage jet flow in bileaflet mechanical heart valves via application of vortex generator arrays. *Journal of biomechanical engineering*, 132(7):071011.
- Naimah, W., Ab, W., Balan, P., Sun, Z., and Miin, Y. (2016). Prediction of thrombus formation using vortical structures presentation in Stanford type B aortic dissection : A preliminary study using CFD approach. *Applied Mathematical Modelling*, 40(4):3115–3127.
- Narracott, A. J., Zervides, C., Diaz, V., Rafiroiu, D., and Lawford, P. V. (2010). Analysis of a mechanical heart valve prosthesis and a native venous valve : Two distinct applications of FSI to biomedical applications. *International Journal for Numerical Methods in Biomedical Engineering*, pages 421–434.
- Nestola, M. G. C., Faggiano, E., Vergara, C., Lancellotti, R. M., Ippolito, S., Filippi, S., Quarteroni, A., and Scrofani, R. (2016). Computational comparison of aortic root stresses in presence of stentless and stented aortic valve bio-prostheses. *Computer Methods in Biomechanics and Biomedical Engineering*, 5842.

- Neumann, I., Santesso, N., Akl, E. A., Rind, D. M., Vandvik, P. O., Alonso-Coello, P., Agoritsas, T., Mustafa, R. A., Alexander, P. E., Schünemann, H., and Others (2016). A guide for health professionals to interpret and use recommendations in guidelines developed with the GRADE approach. *Journal of clinical epidemiology*, 72:45–55.
- Ng, K. C. (2009). A collocated finite volume embedding method for simulation of flow past stationary and moving body. *Computers and Fluids*, 38(2):347–357.
- Nguyen, V. T., Kuan, Y. H., Chen, P. Y., Ge, L., Sotiropoulos, F., Yoganathan, A. P., and Leo, H. L. (2012). Experimentally Validated Hemodynamics Simulations of Mechanical Heart Valves in Three Dimensions. *Cardiovascular Engineering and Technology*, 3(1):88–100.
- Nobari, S., Mongrain, R., Leask, R., and Cartier, R. (2013). The effect of aortic wall and aortic leaflet stiffening on coronary hemodynamic: A fluid-structure interaction study. *Medical and Biological Engineering and Computing*, 51(8):923–936.
- Nobili, M., Morbiducci, U., Ponzini, R., Del Gaudio, C., Balducci, A., Grigioni, M., Maria Montevocchi, F., and Redaelli, A. (2008). Numerical simulation of the dynamics of a bileaflet prosthetic heart valve using a fluid-structure interaction approach. *Journal of biomechanics*, 41(11):2539–2550.
- Noh, W. and Woodward, P. (1976). SLIC (Simple Line Interface Calculation). In *Proceedings of the Fifth International Conference on Numerical Methods in Fluid Dynamics*, pages 330–340.
- OpenFOAM (2014). The Open Source CFD Toolbox, Ver. 2.3.1. <https://openfoam.org/>.
- Paszowski, J. J., Dardik, A., and Haven, N. (2003). Arterial Wall Shear Stress : Observations from the Bench to the Bedside. *Vascular and Endovascular Surgery*, 37(1):47–57.
- Pedrizzetti, G. and Domenichini, F. (2006). Flow-driven opening of a valvular leaflet. *Journal of Fluid Mechanics*, 569:321.
- Pedrizzetti, G. and Domenichini, F. (2007). Asymmetric opening of a simple bileaflet valve. *Physical Review Letters*, 98(21):1–4.
- Pelliccioni, O., Cerrolaza, M., and Herrera, M. (2007). Lattice Boltzmann dynamic simulation of a mechanical heart valve device. *Mathematics and Computers in Simulation*, 75:1–14.
- Peric, M. (1985). *A finite volume method for the prediction of three-dimensional fluid flow in complex ducts*. PhD thesis, Imperial College London (University of London).
- Peskin, C. S. (1972). Flow patterns around heart valves: A numerical method. *Journal of Computational Physics*, 10:252–271.
- Peskin, C. s. (1977). Numerical Analysis of Blood Flow in the Heart. *Journal of Computational Physics*, 25:220–252.

- Peskin, C. S. and McQueen, D. M. (1995). A general method for the computer simulation of biological systems interacting with fluids. In *Symposia of the society for Experimental Biology*, volume 49, pages 265–276. London, England: Syndics of the Cambridge University Press,[1947]-2005.
- Pianet, G. and Arquis, E. (2008). Simulation of particles in fluid: a two-dimensional benchmark for a cylinder settling in a wall-bounded box. *European Journal of Mechanics - B/Fluids*, 27(3):309–321.
- Qin, R. and Krivodonova, L. (2013). A discontinuous Galerkin method for solutions of the Euler equations on Cartesian grids with embedded geometries. *Journal of Computational Science*, 4(1-2):24–35.
- Querzoli, G., Fortini, S., Espa, S., Costantini, M., and Sorgini, F. (2014). Fluid dynamics of aortic root dilation in Marfan syndrome. *Journal of Biomechanics*, 47(12):3120–3128.
- Ravoux, J. F., Nadim, a., and Haj-Hariri, H. (2003). An Embedding Method for Bluff Body Flows: Interactions of Two Side-by-Side Cylinder Wakes. *Theoretical and Computational Fluid Dynamics*, 16(6):433–466.
- Redaelli, A., Bothorel, H., Votta, E., Soncini, M., Morbiducci, U., Del Gaudio, C., Balducci, A., and Grigioni, M. (2004). 3-D simulation of the St. Jude Medical bileaflet valve opening process: fluid-structure interaction study and experimental validation. *The Journal of heart valve disease*, 13(5):804–813.
- Rhie, C.M and Chow, W. (1983). Numerical Study of the Turbulent Flow Past an Airfoil with Trailing Edge Separation.. *AIAA Journal* 21, 11(11):1525–1532.
- Riazuddin, V. N., Zubair, M., Shuaib, I. L., Abdullah, M. Z., Hamid, S. A., and Ahmad, K. A. (2010). Numerical Study of Inspiratory and Expiratory Flow in a Human Nasal Cavity. *Journal of Medical and Biological Engineering*, 31(3):201–206.
- Roache, P. (1994). Perspective: A Method for Uniform Reporting of Grid Refinement Studies. *Journal of Fluids Engineering*, 116:405–413.
- Roache, P. J. (1998). Verification of codes and calculations. *AIAA journal*, 36(5):696–702.
- Robertson, E., Choudhury, V., Bhushan, S., and Walters, D. K. (2015). Validation of OpenFOAM numerical methods and turbulence models for incompressible bluff body flows. *Computers and Fluids*, 123:122–145.
- Roenby, J., Bredmose, H., and Jasak, H. (2016). A Computational Method for Advection, Sharp Interface. *Open Science*, 3(11):160–405.
- Roman, F., Napoli, E., Milici, B., and Armenio, V. (2009). An improved immersed boundary method for curvilinear grids. *Computers and Fluids*, 38(8):1510–1527.
- Romano, G. P. (2008). Deliverable d24-study case report n 2 pulse duplicator with aortic root model from rwth aachen smart-piv ist-2002-37548 European project.Available at <http://www.smart-piv.com>.

- Rosenfeld, M., Avrahami, I., and Einav, S. (2002). Unsteady effects on the flow across tilting disk valves. *Journal of biomechanical engineering*, 124(1):21–29.
- Roudaut, R., Serri, K., and Lafitte, S. (2007). Thrombosis of prosthetic heart valves : diagnosis and therapeutic considerations. *Heart*, 93:137–142.
- Rusche, H. (2002). *Computational Fluid Dynamics of Dispersed Two-Phase Flows at High Phase Fractions*. PhD thesis.
- Saiki, E. M. and S., A. (1996). Numerical Simulation of a Cylinder in Uniform Flow : Application of a Virtual Boundary Method. *Journal of Computational Science*, 465(123):450–465.
- Saxena, R., Lemmon, J., Ellis, J., Yoganathan, A., and Medical, S. J. (2003). An in vitro assessment by means of laser Doppler velocimetry of the Medtronic Advantage bileaflet mechanical heart valve hinge flow. *The Journal of Thoracic and Cardiovascular Surgery*, 126(1):90–98.
- Schafer, M. and Turek, S. (1996). Benchmark Computations of Laminar Flow Around a Cylinder. In *Flow Simulation with High-Performance Computers II*, volume 52, pages 547 – 566.
- Schneider, K. (2014). Approximation of the Laplace and Stokes operators with Dirichlet boundary conditions through volume penalization : a spectral viewpoint. *Numerische Mathematik*, 128(2):301–338.
- Schulz-Heik, K., Ramachandran, J., Bluestein, D., and Jesty, J. (2006). The extent of platelet activation under shear depends on platelet count: differential expression of anionic phospholipid and factor Va. *Pathophysiology of haemostasis and thrombosis*, 34(6):255–262.
- Scotten, L. N. and Walker, D. K. (2004). New laboratory technique measures projected dynamic area of prosthetic heart valves. *The Journal of heart valve disease*, 13(1):120–132.
- Seiler, C. (2004). Management and follow up of prosthetic heart valves. *Heart*, 98:818–824.
- Shadden, S. C., Astorino, M., and Gerbeau, J. F. (2010). Computational analysis of an aortic valve jet with Lagrangian coherent structures. *Chaos*, 20(1):1–10.
- Shahriari, S. (2011). *Computational Modeling of Cardiovascular Flows using Smoothed Particle Hydrodynamics*. PhD thesis.
- Shahriari, S., Maleki, H., Hassan, I., and Kadem, L. (2012). Evaluation of shear stress accumulation on blood components in normal and dysfunctional bileaflet mechanical heart valves using smoothed particle hydrodynamics. *Journal of Biomechanics*, 45(15):2637–2644.
- Sheriff, J., Soared, J. O. S., Xenos, M., Jesty, J., and Bluestein, D. (2013). Evaluation of Shear-Induced Platelet Activation Models Under Constant and Dynamic Shear Stress Loading Conditions Relevant to Devices. *Annals of Biomedical Engineering*, 41(6):1279–1296.

- Shi, Y., Joon, T., Yeo, H., and Zhao, Y. (2006). Particle Image Velocimetry Study of Pulsatile Flow in Bi-leaflet Mechanical Heart Valves with Image Compensation Method. *Journal of biological physics*, 32(6):531–551.
- Shi, Y., Zhao, Y., Yeo, T. J., and Hwang, N. H. (2003). Numerical simulation of opening process in a bileaflet mechanical heart valve under pulsatile flow condition. *The Journal of heart valve disease*, 12(2):245–255.
- Shim, B. and Chang, S. (1997). Numerical Analysis of Three- Dimensional Bjork-Shiley Valvular Flow in an Aorta. *Journal of Biomechanical Engineering*, 119:45–51.
- Shoeb, M. and Fang, M. C. (2013). Assessing bleeding risk in patients taking anticoagulants. *Journal of thrombosis and thrombolysis*, 35(3):312–319.
- Shu, M. C., O'Rourke, K. K., Coppin, C. M., and Lemmon, J. D. (2004). Flow characterization of the ADVANTAGE and St. Jude Medical bileaflet mechanical heart valves. *The Journal of heart valve disease*, 13(5):814–822.
- Silva, L., Silveira-Neto, a., and Damasceno, J. (2003). Numerical simulation of two-dimensional flows over a circular cylinder using the immersed boundary method. *Journal Of Computational Physics*, 189(2):351–370.
- Simon, H., Liang, G., Fotis, S., and P., Y. A. (2010a). Simulation of the three-dimensional hinge flow fields of a bileaflet mechanical heart valve under aortic conditions. *Annals of Biomedical Engineering*, 38(3):841–853.
- Simon, H. A. (2009). *Numerical Simulations of the Micro Flow Field in the Hinge Region*. PhD thesis, Georgia Institute of Technology.
- Simon, H. A., Ge, L., Sotiropoulos, F., and Yoganathan, A. P. (2010b). Numerical investigation of the performance of three hinge designs of bileaflet mechanical heart valves. *Annals of Biomedical Engineering*, 38(11):3295–3310.
- Sirois, E. and Sun, W. (2011). Computational evaluation of platelet activation induced by a bioprosthetic heart valve. *Artificial organs*, 35(2):157–165.
- Smadi, O., Fenech, M., Hassan, I., and Kadem, L. (2009). Flow through a defective mechanical heart valve : A steady flow analysis. *Medical engineering & physics*, 31(3):295–305.
- Soares, J. S., Sheriff, J., and Bluestein, D. (2013). A novel mathematical model of activation and sensitization of platelets subjected to dynamic stress histories. *Biomech ModelMechanobiol*, 12(6):1127–1141.
- Sotiropoulos, F., Bao Le, T., and Gilmanov, A. (2016). Fluid Mechanics of Heart Valves and Their Replacements. *Annual Review of Fluid Mechanics*, 48:259–283.
- Sotiropoulos, F. and Borazjani, I. (2009). A review of state-of-the-art numerical methods for simulating flow through mechanical heart valves. *Medical & biological engineering & computing*, 47(3):245–256.

- Sotiropoulos, F. and Yang, X. (2014). Immersed boundary methods for simulating fluid-structure interaction. *Progress in Aerospace Sciences*, 65:1–21.
- Stefano, Z., Formaggia, L., and Vergara, C. (2016). An unfitted formulation for the interaction of an incompressible fluid with a thick structure via an XFEM / DG approach. *MOX Report n. 35/2016*, (35).
- Stern, F., Wilson, R., and Shao, J. (2006). Quantitative V&V of CFD simulations and certification of CFD codes. *International Journal for Numerical methods in Fluids*, 50(11):1335–1355.
- Stern, F., Wilson, R. V., Coleman, H. W., and Paterson, E. G. (2001). Comprehensive Approach to Verification and Validation of CFD Simulations Part 1: Methodology and Procedures. *Journal of Fluids Engineering*, 123(4):793.
- Stijnen, J. M. A., de Hart, J., Bovendeerd, P. H. M., and van de Vosse, F. N. (2004). Evaluation of a fictitious domain method for predicting dynamic response of mechanical heart valves. *Journal of Fluids and Structures*, 19(6):835–850.
- Sturla, F., Votta, E., Stevanella, M., Conti, C. A., and Redaelli, A. (2013). Impact of modeling fluidstructure interaction in the computational analysis of aortic root biomechanics. *Medical Engineering and Physics*, 35(12):1721–1730.
- Su, B., Kabinejadian, F., Phang, H. Q., Kumar, G. P., Cui, F., Kim, S., Tan, R. S., Hon, J. K. F., Allen, J. C., Leo, H. L., and Zhong, L. (2015). Numerical modeling of intraventricular flow during diastole after implantation of BMHV. *PLoS ONE*, 10(5).
- Su, S.-w., Lai, M.-c., and Lin, C.-a. (2007). An immersed boundary technique for simulating complex flows with rigid boundary. *Computers & Fluids*, 36:313–324.
- Sugiyama, K., Ii, S., Takeuchi, S., Takagi, S., and Matsumoto, Y. (2011). A full Eulerian finite difference approach for solving fluidstructure coupling problems. *Journal of Computational Physics*, 230(3):596–627.
- Sun, W., Li, K., and Sirois, E. (2010). Simulated elliptical bioprosthetic valve deformation: implications for asymmetric transcatheter valve deployment. *Journal of biomechanics*, 43(16):3085–3090.
- Suo, J. (2005). *Investigation of blood flow patterns and hemodynamics in the human ascending aorta and major trunks of right and left coronary arteries using magnetic resonance imaging and computational fluid dynamics*. PhD thesis, Georgia Institute of Technology.
- Tai, C. H., Liew, K. M., and Zhao, Y. (2007). Numerical simulation of 3D fluid-structure interaction flow using an immersed object method with overlapping grids. *Computers and Structures*, 85(11-14):749–762.
- Takagi, S., Sugiyama, K., Ii, S., and Matsumoto, Y. (2012). A Review of Full Eulerian Methods for Fluid Structure Interaction Problems. *Journal of Applied Mechanics*, 79(1):010911.

- Tamagawa, M., Kaneda, H., Hiramoto, M., and Nagahama, S. (2009). Simulation of Thrombus Formation in Shear Flows Using Lattice Boltzmann Method. *Artificial Organs*, 33(8):604–610.
- Tanaka, H. and Araki, T. (2000). Simulation method of colloidal suspensions with hydrodynamic interactions: fluid particle dynamics. *Physical Review Letters*, 85(6):1338–1341.
- Tang, H. S., Jones, S. C., and Sotiropoulos, F. (2003). An overset-grid method for 3D unsteady incompressible flows. *Journal of Computational Physics*, 191(2):567–600.
- Teijeira, F. J. and Mikhail, A. A. (1992). *Cardiac Valve Replacement with Mechanical Prostheses: Current Status and Trends*, pages 197–227. Springer US, Boston, MA.
- Tse, K. M., Chiu, P., Lee, H. P., and Ho, P. (2011). Investigation of hemodynamics in the development of dissecting aneurysm within patient-specific dissecting aneurismal aortas using computational fluid dynamics (CFD) simulations. *Journal of Biomechanics*, 44(5):827–836.
- Tseng, Y.-h. and Ferziger, J. H. (2003). A ghost-cell immersed boundary method for flow in complex geometry. *Journal of Computational Physics*, 192:593–623.
- Tullio, M. D. D., Nam, J., Pascasio, G., Balaras, E., and Verzicco, R. (2012). Computational prediction of mechanical hemolysis in aortic valved prostheses. *European Journal of Mechanics B/Fluids*, 35:47–53.
- Van Loon, R., Anderson, P., and van de Vosse, F. (2006). A fluid-structure interaction method with solid-rigid contact for heart valve dynamics. *Journal of Computational Physics*, 217(2):806–823.
- Van Loon, R., Anderson, P. D., de Hart, J., and Baaijens, F. P. T. (2004). A combined fictitious domain/adaptive meshing method for fluidstructure interaction in heart valves. *International Journal for Numerical Methods in Fluids*, 46(5):533–544.
- Vanella, M. and Balaras, E. (2009). Short Note A moving-least-squares reconstruction for embedded-boundary formulations. *Journal of Computational Physics*, 228(18):6617–6628.
- Vergara, C., Viscardi, F., Antiga, L., and Luciani, G. B. (2012). Influence of Bicuspid Valve Geometry on Ascending Aortic Fluid Dynamics: A Parametric Study. *Artificial Organs*, 36(4):368–378.
- Versteeg, H. K. and Malalasekera, W. (2007). *An introduction to computational fluid dynamics: the finite volume method*. Pearson Education.
- Vierendeels, J., Dumont, K., Dick, E., and Verdonck, P. (2005). Analysis and Stabilization of Fluid-Structure Interaction Algorithm for Rigid-Body Motion. *AIAA Journal*, 43(12):2549–2557.
- Vigmostad, S. C. and Udaykumar, H. S. (2011). Algorithms for FluidStructure Interaction. In Chandran, K. B., Udaykumar, H. S., and Reinhardt, J. M., editors, *Image-Based Computational Modeling of the Human Circulatory and Pulmonary Systems*, pages 191–234. Springer US, Boston, MA.

- Vitale, N., De Feo, M., De Santo, L. S., Pollice, A., Tedesco, N., and Cotrufo, M. (1999). Dose-dependent fetal complications of warfarin in pregnant women with mechanical heart valves. *Journal of the American College of Cardiology*, 33(6):1637–1641.
- Voller, V. R. and Prakash, C. (1987). A fixed grid numerical modeling methodology for convection-diffusion mushy region phase-change problems. *International Journal of Heat and Mass Transfer*, 30(8):1709–1987.
- Votta, E., Le, T. B., Stevanella, M., Fusini, L., Caiani, E. G., Redaelli, A., and Sotiropoulos, F. (2013). Toward patient-specific simulations of cardiac valves: state-of-the-art and future directions. *Journal of biomechanics*, 46(2):217–28.
- Wang, W. (2009). *A non-body conformal grid method for simulations of laminar and turbulent flows with a compressible large eddy simulation solver*. Graduate theses and dissertations, Iowa State University.
- Weller, H. G. (2008). A new approach to VOF-based interface capturing methods for incompressible and compressible flow. *OpenCFD Ltd., Report TR/HGW/04*.
- Wendell, D. C., Samyn, M. M., Cava, J. R., Ellwein, L. M., Krolikowski, M. M., Gandy, K. L., Pelech, A. N., Shadden, S. C., and LaDisa, J. F. (2012). Including aortic valve morphology in computational fluid dynamics simulations: Initial findings and application to aortic coarctation.
- Wilcox, D. C. (1994). Simulation of Transition with a Two-Equation Turbulence Model. *AIAA Journal*, 32(2).
- Wilson, R. V., Coleman, H. W., and Paterson, E. G. (2001). Comprehensive Approach to Verification and Validation of CFD Simulations Part 2 : Application for Rans Simulation of a Cargo / Container Ship. 123(December 2001):803–810.
- Woo, Y. R. and Yoganathan, A. P. (1984). Two-component laser Doppler anemometer for measurement of velocity and turbulent shear stress near prosthetic heart valves. *Medical instrumentation*, 19(5):224–231.
- Woo, Y.-R. and Yoganathan, A. P. (1986a). In vitro pulsatile flow velocity and shear stress measurements in the vicinity of mechanical mitral heart valve prostheses. *Journal of biomechanics*, 19(1):39–51.
- Woo, Y.-R. and Yoganathan, A. P. (1986b). Pulsatile flow velocity and shear stress measurements on the St. Jude bileaflet valve prosthesis. *Scandinavian journal of thoracic and cardiovascular surgery*, 20(1):15–28.
- Woo, Y.-R. and Yoganathan, A. P. (1986c). Pulsatile flow velocity and shear stress measurements on the St. Jude bileaflet valve prosthesis. *Scandinavian journal of thoracic and cardiovascular surgery*, 20(1):15–28.
- Wu, J., Yun, B. M., Fallon, A. M., Hanson, S. R., Aidun, C. K., and Yoganathan, A. P. (2011). Numerical Investigation of the Effects of Channel Geometry on Platelet Activation and Blood Damage. *Annals of biomedical engineering*, 39(2):897–910.

- Xenos, M., Girdhar, G., Alemu, Y., Jesty, J., Slepian, M., Einav, S., and Bluestein, D. (2010). Device Thrombogenicity Emulator (DTE) - Design optimization methodology for cardiovascular devices: A study in two bileaflet MHV designs. *Journal of Biomechanics*, 43(12):2400–2409.
- Xia, G. H., Zhao, Y., and Yeo, J. H. (2009). Parallel unstructured multigrid simulation of 3D unsteady flows and fluid-structure interaction in mechanical heart valve using immersed membrane method. *Computers and Fluids*, 38(1):71–79.
- Xu, S. (2008). The immersed interface method for simulating prescribed motion of rigid objects in an incompressible viscous flow. *Journal of Computational Physics*, 227(10):5045–5071.
- Yang, J. (2016). Sharp interface direct forcing immersed boundary methods : A summary of some algorithms and applications. *Journal of Hydrodynamics*, 28(5):713–730.
- Yang, J. and Balaras, E. (2006). *An embedded-boundary formulation for large-eddy simulation of turbulent flows interacting with moving boundaries*. PhD thesis, University of Minnesota.
- Yin, W., Alemu, Y., Affeld, K., Jesty, J., and Bluestein, D. (2004). Flow-induced platelet activation in bileaflet and monoleaflet mechanical heart valves. *Annals of Biomedical Engineering*, 32(8):1058–1066.
- Yoganathan, A. P. (2000). Yoganathan, A. P. Cardiac Valve Prostheses.. In Bronzino, E. J. D., editor, *The Biomedical Engineering Handbook: Second Edition*, chapter 127. Boca Raton: CRC Press LLC, second edi edition.
- Yoganathan, A. P., Chaux, A., Gray, R. J., Woo, Y.-R., DeRobertis, M., Williams, F. P., and Matloff, J. M. (1984). Bileaflet , Tilting Disc and Porcine Aortic Valve Substitutes : In Vitro. *Journal of the American College of Cardiology*, 3(2):313–320.
- Yoganathan, a. P., He, Z., and Casey, J. S. (2004). Fluid mechanics of heart valves. *Annual Review of Biomedical Engineering*, 6:331–362.
- Yokoi, K., Xiao, F., Liu, H., and Fukasaku, K. (2005). Three-dimensional numerical simulation of flows with complex geometries in a regular Cartesian grid and its application to blood flow in cerebral artery with multiple aneurysms. *Journal of Computational Physics*, 202(1):1–19.
- Yoshizawa, A. and Horiuti, K. (1985). A statistically-derived subgrid-scale kinetic energy model for the large-eddy simulation of turbulent flows. *Journal of the Physical Society of Japan*, 54(8):2834–2839.
- Yu, Y., Baek, H., and Karniadakis, G. E. (2013). Generalized fictitious methods for fluid-structure interactions: Analysis and simulations. *Journal of Computational Physics*, 245:317–346.
- Yun, B. M., Aidun, C. K., and Yoganathan, A. P. (2014a). Blood Damage Through a Bileaflet Mechanical Heart Valve: A Quantitative Computational Study Using a Multi-scale Suspension Flow Solver. *Journal of Biomechanical Engineering*, 136(10):17.

- Yun, B. M., Dasi, L. P., Aidun, C. K., and Yoganathan, a. P. (2014b). Computational modelling of flow through prosthetic heart valves using the entropic lattice-Boltzmann method. *Journal of Fluid Mechanics*, 743:170–201.
- Yun, B. M., Dasi, L. P., Aidun, C. K., and Yoganathan, a. P. (2014c). Highly resolved pulsatile flows through prosthetic heart valves using the entropic lattice-Boltzmann method. *Journal of Fluid Mechanics*, 754:122–160.
- Yun, B. M., McElhinney, D. B., Arjunon, S., Mirabella, L., Aidun, C. K., and Yoganathan, A. P. (2014d). Computational simulations of flow dynamics and blood damage through a bileaflet mechanical heart valve scaled to pediatric size and flow. *Journal of Biomechanics*, 47(12):3169–3177.
- Yun, B. M., Wu, J., Simon, H. A., Arjunon, S., Sotiropoulos, F., Aidun, C. K., and Yoganathan, A. P. (2012). A numerical investigation of blood damage in the hinge area of aortic bileaflet mechanical heart valves during the leakage phase. *Annals of Biomedical Engineering*, 40(7):1468–1485.
- Zakaria, M. S., Ismail, F., Tamagawa, M., Fazli, A., Aziz, A., Wiriadidjaya, S., Basri, A. A., and Ahmad, K. A. (2016). Numerical Analysis Using a Fixed Grid Method for Cardiovascular Flow Application. *Journal of Medical Imaging and Health Informatics*, 6(6):1483–1488.
- Zakaria, M. S., Osman, K., Saadun, M. N. A., Manaf, M. Z. A., Hanafi, M., and Hafidzal, M. (2013). Computational Simulation of Boil-Off Gas Formation inside Liquefied Natural Gas tank using Evaporation Model in ANSYS Fluent. In *Applied Mechanics and Materials*, volume 393, pages 839–844. Trans Tech Publ.
- Zalesak, S. T. (1979). Fully multidimensional flux-corrected transport algorithms for fluids. *Journal of Computational Physics*, 31(3):335–362.
- Zhen, T. K., Zubair, M., and Ahmad, K. A. (2011). Experimental and Numerical Investigation of the Effects of Passive Vortex Generators on Aludra UAV Performance. *Chinese Journal of Aeronautics*, 24(5):577–583.